Check for updates

Received: 9 April 2021 | Revised: 28 February 2022 | Accepted: 6 March 2022

DOI: 10.1111/geb.13515

RESEARCH ARTICLE

Global Ecology and Biogeography A Journal of Macroecology WILEY

# Global estimates of the extent and production of macroalgal forests

Carlos M. Duarte[1,2] | Jean-Pierre Gattuso[3,4] | Kasper Hancke[5] | Hege Gundersen[5] | Karen Filbee-Dexter[6,7] | Morten F. Pedersen[8] | Jack J. Middelburg[9] | Michael T. Burrows[10] | Kira A. Krumhansl[11] | Thomas Wernberg[7,12] | Pippa Moore[12] | Albert Pessarrodona[12] | Sarah B. Ørberg[2,13] | Isabel S. Pinto[14] | Jorge Assis[15] | Ana M. Queirós[16] | Dan A. Smale[17] | Trine Bekkby[5] | Ester A. Serrão[15] | Dorte Krause-Jensen[2,13]

[1]Red Sea Research Center, King Abdullah University of Science and Technology (KAUST), Thuwal, Saudi Arabia

[2]Arctic Research Centre, Aarhus University, Århus C, Denmark

[3]Laboratoire d'Océanographie de Villefranche, Sorbonne Université, CNRS, Villefranche-sur-mer, France

[4]Institute for Sustainable Development and International Relations, Sciences Po, Paris, France

[5]Norwegian Institute for Water Research (NIVA), Oslo, Norway

[6]Institute of Marine Research, His, Norway

[7]UWA Oceans Institute & School of Biological Sciences, University of Western Australia, Crawley, Western Australia, Australia

[8]Department of Science and Environment, Roskilde University, Roskilde, Denmark

[9]Department of Earth Sciences, Utrecht University, Utrecht, The Netherlands

[10]Scottish Association for Marine Science, Scottish Marine Institute, Oban, UK

[11]Fisheries and Oceans Canada, Bedford Institute of Oceanography, Dartmouth, Nova Scotia, Canada

[12]Institute of Biological, Environmental and Rural Sciences, Aberystwyth University, Aberystwyth, UK

[13]Department of Bioscience, Aarhus University, Silkeborg, Denmark

[14]Ciimar/CIMAR and Faculty of Sciences, University of Porto, Porto, Portugal

[15]CCMAR, Universidade do Algarve, Campus de Gambelas, Faro, Portugal

[16]Plymouth Marine Laboratory, Plymouth, UK

[17]Marine Biological Association of the United Kingdom, Plymouth, UK

**Correspondence**
Carlos M. Duarte, Red Sea Research Center, King Abdullah University of Science and Technology (KAUST), Thuwal 23955-6900, Saudi Arabia.
Email: carlos.duarte@kaust.edu.sa

**Funding information**
Research for this paper was supported by Euromarine (http://www.euromarinenetwork.eu). We also received support from FCT – Foundation for Science and Technology through project UIDB/04326/2020 and the transitional norm – DL57/2016/CP1361/CT0035. JA and EAS received support from FCT

## Abstract

**Aim:** Macroalgal habitats are believed to be the most extensive and productive of all coastal vegetated ecosystems. In stark contrast to the growing attention on their contribution to carbon export and sequestration, understanding of their global extent and production is limited and these have remained poorly assessed for decades. Here we report a first data-driven assessment of the global extent and production of macroalgal habitats based on modelled and observed distributions and net primary production (NPP) across habitat types.

**Location:** Global coastal ocean.

**Time period:** Contemporary.

This is an open access article under the terms of the Creative Commons Attribution-NonCommercial-NoDerivs License, which permits use and distribution in any medium, provided the original work is properly cited, the use is non-commercial and no modifications or adaptations are made.
© 2022 The Authors. *Global Ecology and Biogeography* published by John Wiley & Sons Ltd.

– Foundation for Science and Technology (Portugal) through UIDB/04326/2020, SFRH/BSAB/150485/2019, and the transitional norm – DL57/2016/CP1361/CT0035 as well as project MARFOR (Biodiversa/0004/2015) and a Pew Marine Fellowship. J-PG received support from Prince Albert II of Monaco Foundation, Veolia Foundation, IAEA Ocean Acidification International Coordination Centre and French Facility for Global Environment. DK-J received support from the Independent Research Fund Denmark through the project 'CARMA' (reference: 8021-00222B). AMQ acknowledges funding support from UKRI GCRF Blue Communities. JJM was supported by the Netherlands Earth System Science Centre. HG, KH and TB received funds from KELPPRO (RCN #267536), Nordic Blue Carbon (NEA #17080044), OPTIMAKELP (NFR #280732), and STORISK project (ANR-15-CE03-0003). TW was supported by the Australian Research Council (DP170100023). DAS was supported by a UKRI Future Leaders Fellowship (MR/S032827/1). KF-D was supported by the Norwegian Blue Forest Network. PM was supported by a NERC/Newton Fund Latin American Biodiversity Programme NE/SO11692/1.

**Handling Editor:** Richard Field

**Major taxa studied:** Macroalgae.

**Methods:** Here we apply a comprehensive niche model to generate an improved global map of potential macroalgal distribution, constrained by incident light on the seafloor and substrate type. We compiled areal net primary production (NPP) rates across macroalgal habitats from the literature and combined this with our estimates of the global extent of these habitats to calculate global macroalgal NPP.

**Results:** We show that macroalgal forests are a major biome with a global area of 6.06–7.22 million km$^2$, dominated by red algae, and NPP of 1.32 Pg C/year, dominated by brown algae.

**Main conclusions:** The global macroalgal biome is comparable, in area and NPP, to the Amazon forest, but is globally distributed as a thin strip around shorelines. Macroalgae are expanding in polar, subpolar and tropical areas, where their potential extent is also largest, likely increasing the overall contribution of algal forests to global carbon sequestration.

**KEYWORDS**
area, biome, macroalgae, niche, production, seaweeds, trends

## 1 | INTRODUCTION

Coastal vegetated habitats are currently in the global focus because of their capacity to support substantial carbon sequestration (Duarte et al., 2013; Krause-Jensen & Duarte, 2016; Macreadie et al., 2019; Serrano et al., 2019). However, the role of macroalgae as blue carbon habitats had been neglected for decades on the grounds that they predominantly grow on rocky shores, which do not accumulate carbon (Krause-Jensen et al., 2018; Nellemann et al., 2009). Growing evidence for the globally relevant carbon export and sequestration from wild macroalgae (Krause-Jensen & Duarte, 2016; Ortega et al., 2019), along with possible contributions from large-scale farmed macroalgae, unique among coastal vegetated habitats, is raising awareness of the potential role of macroalgal habitats in climate change mitigation (Duarte et al., 2017; Froehlich et al., 2019).

Macroalgal forests, a term we use hereafter to refer to macroalgal-dominated habitats in general, are important habitats that add structural complexity and allow the co-existence of a high diversity of species (Steneck et al., 2002; Teagle et al., 2017). Macroalgae are broadly distributed, occurring across all coastlines and oceans. They consist of brown algae, such as large canopy-forming kelps and intertidal fucoids, red algae and green algae. They occur from the intertidal zone to the greatest depths (> 200 m) receiving enough light to support their growth. This varies across functional forms, with crustose red algae having the lowest average light requirements among macroalgal types (Gattuso et al., 2006; Markager & Sand-Jensen, 1992). Many macroalgae require hard substrates to anchor to the seafloor and occur predominantly on bedrock, boulders, cobbles or biogenic structures (e.g. mussels, corals), while others are able to attach to soft sediments (e.g. *Halimeda*, *Caulerpa*) or may occur free-floating (e.g. *Sargassum natans* and *Sargassum fluitans*).

The high production of macroalgal forests supports food webs locally as well as at distant sites receiving their exported production (Krumhansl & Scheibling, 2012; Pessarrodona et al., 2018; Queirós et al., 2019). Food webs in macroalgal-dominated systems support highly productive commercial and recreational coastal fisheries (Bennett et al., 2016; Blamey & Bolton, 2018; Melis et al., 2019) The intense photosynthetic activity and attenuation of solar radiation by algal forests provide local refugia to vulnerable biota from elevated UV radiation and ocean acidification (Krause-Jensen et al., 2016; Wahl et al., 2018) and, in the case of intertidal fucoid canopies, from daily thermal extremes (Bulleri et al., 2018). Moreover, local reduction of currents by algal canopies protects shores from erosion and increases the local retention of organic matter (Estes & Palmisano, 1974; Løvås & Tørum, 2001).

The growing attention to the roles of macroalgal habitats is, however, in stark contrast to our poor understanding of their global extent and production, and the changes they are undergoing (Duarte, 2017; Wernberg et al., 2019). This is a major limitation, since macroalgal forests are believed to form the most extensive and productive habitats of all coastal vegetated ecosystems (Duarte, 2017;

Duarte & Cebrián, 1996; Smith, 1981). Macroalgal production varies across populations and communities, as well as with resource (light and nutrients) supply, hydrodynamic conditions (waves and currents) and herbivory (Bustamante et al., 1995; Carpenter et al., 1991; Castorani et al., 2021). The resulting net primary production (NPP) per unit area of many macroalgal stands ranks among the highest of any habitat in the world, rivalling that of tropical rain forests (Pace & Lovett, 2013).

Estimates of the global extent of macroalgae range from an early unsupported value of $0.6 \times 10^6$ km$^2$ (Whittaker & Likens, 1973) to a maximum of $12.5 \times 10^6$ km$^2$ constrained by sufficient light availability at the seafloor, based on the first decile of minimum light requirements for growth, excluding Antarctica (Gattuso et al., 2006), and with an average at around $3.54 \times 10^6$ km$^2$ (Krause-Jensen & Duarte, 2016). Reported estimates of global macroalgal NPP range 20-fold from 0.13 to 2.9 Pg C/year, calculated as the product of area estimates and the mean NPP per unit area of around 0.4 kg C/m$^2$/year (Duarte, 2017; Duarte & Cebrián, 1996; Krause-Jensen & Duarte, 2016).

The huge uncertainties surrounding the global area covered and the global NPP of macroalgal habitats have not been constrained further over the past 50 years, with the global estimates available resting largely on guess work and very thin datasets propagated for decades across citation chains without being improved, so they should be considered tentative at best (Duarte, 2017). Yet, there has been, in parallel, a huge growth in the number of published reports and observations of macroalgal distribution and production available, relative to the thin datasets upon which previous estimates of global area and production were based. Hence, failure to update global estimates using the wealth of observations now available unnecessarily perpetuates an unacceptable knowledge gap in a globally significant component of the ocean ecosystem and the carbon cycle it supports (Duarte, 2017).

Distribution models predicting the likelihood of occurrence of macroalgae have since been refined further at the regional scale to include higher resolution climate, bathymetry and light estimates, along with other factors constraining the occurrence of macroalgae, such as seafloor type and wave exposure. These refined models have been used to identify areas with high probability of occurrence of kelp forests along the coasts of the north-east Atlantic (Assis, Araújo, et al., 2018), the north-east Pacific (Gregr et al., 2019), eastern Canada (Filbee-Dexter, 2016), Australia (Martínez et al., 2018; Young et al., 2015), the UK (Burrows et al., 2018), and north-western France (Gorman et al., 2013), as well as of other seaweed types such as fucoids in the Mediterranean and Atlantic (Buonomo et al., 2018; Neiva et al., 2014). However, this approach has not yet been used to predict distributions at global scales.

Consequently, there is a need and an opportunity to narrow the order-of-magnitude of uncertainty on the global extent and production of macroalgal forests. Moreover, existing estimates are rooted in insufficient appreciation of the diversity of habitats where macroalgae grow, which include rocky shores, soft sediments and even the open ocean.

Here we provide improved estimates of the global area occupied by macroalgae and the primary production they support across different habitat types. We do so on the basis of three complementary approaches for estimating the global macroalgal area. The first approach estimates the upper boundary of the area suitable for macroalgal growth on the basis of a global niche model. The second approach estimates the upper boundary for the area of rocky shore macroalgae can occupy by simply quantifying the area of rocky shores shallower than 50 m. The third, more detailed, approach provides a global estimate of macroalgal area based on the sum of area estimates for macroalgal habitat types, including rocky shore habitat, soft-bottom habitat and floating habitats. We then combined the resulting habitat-specific estimates of global macroalgal area with the average of reported NPP estimates for these habitats to yield an estimate of habitat-specific NPP and, by accumulating them across habitats, a global estimate of macroalgal NPP.

## 2 | METHODS

### 2.1 | Estimating the global macroalgal area

#### 2.1.1 | Global niche model (approach 1)

Niche models were used to estimate the global potential distribution of brown and red macroalgal species, modelled by combining information on habitat requirements for red and brown algae species. We first extended the approach of Gattuso et al. (2006) by including habitat requirements for macroalgae in addition to light, specifically high-resolution spatial thresholds of ocean temperature, salinity, ice extent and nutrients (cf. Duarte et al., 2021 for the data layers on predicted macroalgal occurrence). These thresholds identified regions with suitable niche conditions by crossing empirical physiological information known to shape the distribution of seaweed species, alongside with high-resolution environmental gradients produced at global scales (Kearney & Porter, 2009). Environmental layers with high spatial resolution were produced to model the distribution of both intertidal and subtidal algal forests. This used the interpolation method detailed in Assis, Araújo, et al. (2018) and Assis, Serrão, et al. (2018) with the new General Bathymetric Chart of the Oceans (GEBCO) (https://www.gebco.net/, 2019 update), to provide standardized sea surface layers with a 15 arc-second resolution (approx. 450 m at the equator) of temperature, salinity, nitrate and ice thickness, as well as along-bottom layers of temperature, salinity, nitrate and light availability. The data used in the interpolation were the Global Observed Ocean Physics Reprocessing, the Global Ocean Physics Reanalysis and the Global Ocean Biogeochemistry Non-assimilative Hindcast, all with native spatial resolutions of 15 arc-minute resolution, temporal resolutions from 2000 to 2015, and available from the Copernicus data service (see Assis, Araújo, et al. (2018) and Assis, Serrão, et al. (2018) for more details).

Data on environmental requirements for species of brown algae (Ochrophyta, Phaeophyceae) and red algae (Rhodophyta) were

compiled from the available literature. This depended on whether species were intertidal or subtidal and on the availability of environmental layers at global scales. For intertidal species, data compiled considered sea surface temperature, salinity and nutrients (such as nitrates) and seasonal sea ice thickness (e.g. Assis et al., 2014; Song et al., 2021) while for subtidal species the compiled data included ocean temperature, salinity, nutrients and light availability at the sea bottom, as well as permanent sea ice thickness (e.g. Assis et al., 2017). Among the range of tolerance limits found per variable, the 95th percentile thresholds were used as extreme proxies for cross-taxa environmental requirements (cf. Table S2 for the environmental requirements shaping the distribution of different macroalgal groups).

Threshold niche models were developed by reclassifying the environmental gradients to binomial surfaces (1: suitable; 0: unsuitable) using the physiological thresholds inferred for the different seaweed groups. A product function was applied to these surfaces (Table S3) to identify regions of agreement where suitable niche conditions can be found. A global layer of intertidal habitats was further computed by determining the regions above the hydrographical zero, within the range of tidal amplitude (e.g. Assis et al., 2014). This approach used the new GEBCO with the amplitude constituent of the Hamburg direct data Assimilation Methods for TIDEs model (Taguchi et al., 2014).

The final threshold outputs were used to produce maps of potential distribution and to estimate global distribution areas. The intertidal layer was further used to discriminate between intertidal and subtidal areas to yield upper boundary area estimates (Table 1).

### 2.1.2 | Upper limit of distribution of rocky macroalgae constrained by the area of rocky shores shallower than 50 m (approach 2)

The potential maximum extent of macroalgae distribution on rocky shores (Figure 1b) was calculated as rocky seafloor area shallower than 50 m, which contains the majority of the areas with light conditions suitable for macroalgae growth over suitable substrate (i.e. rocky bottom). Information on depth came from the GEBCO gridded bathymetric data (https://www.gebco.net/, GEBCO, 2019), which is a global terrain model for ocean and land at 15 arc-second intervals. The derived polygons of suitable light conditions were assigned to the world's countries by linking them to a world map of the Exclusive Economic Zones (EEZ). To be able to calculate the approximate proportion of these areas (having sufficient light) having suitable substrate, the percentage of rocky seabed was estimated for each polygon based on percentage of the seabed along the shoreline of nations dominated by hard rocks, conglomerates, and rocky shores (Young & Carilli, 2019). This is an oversimplification as it only provides estimates at national scales, but represents the best global estimate available. If an estimate was lacking for a country in the dataset of Young and Carilli (2019), the estimate was selected from the neighbouring islands or by assigning averaged values from neighbouring countries.

To validate the global map of the maximum extent of macroalgal distribution (presented in Figure 1b), we needed to assess the reliability of the assumption that we could use the percentage of rocky seabed provided by Young and Carilli (2019) also in the subtidal areas further off the shore as an approximation of the percentage of areas having suitable substrate. To be able to do this, we used data from mapping programs from countries for which substrate mapping was considered to have good coverage (assessed by source personnel delivering the data). Data from the UK, Ireland, Spain (without the Canary Islands), Portugal (without the Azores and Madeira), France, Denmark and Finland were received from European Marine Observation and Data Network (EMODnet) Seabed Habitats (14 December 2021 for the UK, 1 December 2020 for the other countries, EMODnet contact person: Elenora Manca, Joint Nature Conservation Committee). These layers were produced using data from EMODnet geology maps at 1:100,000 and 1:250,000 scales (Populus et al., 2017). Data from New Zealand were based on the New Zealand Sea Bed database, which includes data from ~150 published, unpublished, national and international collections covering more than 30,000 sediment analyses and observations (Bostock et al., 2018). Bedrock, boulders and rocks were considered to be substrate types suitable for macroalgae growth and were therefore included in the dataset. The size of the rocky seabed area provided by this evaluation dataset and the size of the modelled rocky seabed, obtained by multiplying the size of the area with depths shallower than 50 m with the rock fraction is presented for each country in Table S4. From these data, the fraction of the mapped versus the modelled size was calculated (Table S4). This number varied between countries, but was on average 90% ($SD = 65\%$), meaning that overall, the size of the observed rocky seabed (from the validation dataset) was 90% of what was modelled. This was used to correct the area of the upper limit to macroalgal area on rocky shores from $5.4 \times$ to $4.9 \times 10^6$ km$^2$. This approach complements that based on niche models, as substrate type was not available in the global environmental datasets available to develop niche models.

### 2.1.3 | Global estimate of macroalgae based on the sum of area estimates for macroalgal habitat types (approach 3)

Improved assessments of the global macroalgael area can be delivered by aggregating separate estimates for different macroalgal habitat types. Rocky intertidal habitats along temperate and polar coastlines are generally dominated by brown algae, specifically Fucales, such as *Fucus* spp. in the Northern and *Durvillaea* spp. in the Southern Hemisphere. In the subtidal zone, large canopy forming Laminariales, which include most kelps, are found along ~25% of the world's coastlines (Wernberg et al., 2019), and typically extend to depths of 30–40 m, and exceptionally down to 60–80 m (Assis, Serrão, et al., 2018; Graham et al., 2007; Krause-Jensen et al., 2019),

**TABLE 1** Estimates of the global macroalgal area: existing published estimates of total area, updated estimates of the upper boundary of total macroalgal area and updated estimates of macroalgal areas by habitat type including rocky habitats, soft/sandy habitats and floating habitats and the total area of these. Details in Methods and in Table S1 (estimates based on literature compilation)

| Published estimates of macroalgal cover | Global area ($10^6$ $Km^2$) | Reference, overall approach |
|---|---|---|
| Upper boundary of benthic habitats | 13.3 | Gattuso et al. (2006) |
| | 12.5 | Gattuso et al. (2020) |
| Mean (range: 25–75% percentiles) of literature data | 3.54 (2.8–4.28) | Krause-Jensen and Duarte (2016) |
| Global modelled estimates – Approach 1 | | |
| Intertidal brown algae | 0.13 | Global niche modelling approach, this study, independent of light threshold |
| Subtidal brown algae | 2.50 | Global niche modelling approach, this study, light threshold: first decile compensation irradiance (Ec) growth (Gattuso et al., 2006) |
| Intertidal red algae | 0.40 | Global niche modelling approach, this study, independent of light threshold |
| Subtidal red algae (all) | 6.69 | Global niche modelling approach, this study, light threshold: first decile Ec growth (Gattuso et al., 2006) |
| Subtidal red algae beyond brown algal belt | 4.19 | Global niche modelling approach, this study, light threshold: first decile Ec growth (Gattuso et al., 2006), after removing the area occupied by brown algae |
| Total macroalgal area – upper boundary | 7.22 | Overall estimate of brown and red algae |
| Rocky shore area within 50 m depth (Approach 2) | 4.9 | Based on bathymetry and the fraction of shoreline that is rocky (.52, Young & Carilli, 2019), validated in this study (cf. Figure 1b, Methods and Table S4) |
| Estimates by habitat type (Approach 3) | | |
| Macroalgae on rocky habitat | | |
| Intertidal communities | 0.013 | Intertidal area ($0.128 \times 10^6$ $km^2$, Murray et al., 2019) multiplied by rocky shore fraction (.52, Young & Carilli, 2019) and assumed fraction of algal cover (.20). |
| Subtidal brown algae | 1.68 (1.43–1.79) | Global correlative niche modelling approach, multiplied by the fraction of shoreline that is rocky (0.52, Young & Carilli, 2019), minus the estimated area of intertidal algae. Range of estimates in parentheses. |
| Subtidal red algae beyond brown algae | 2.98 | Upscaled from the ratio of the area of red algae growing at depths greater than the belt of brown algae, to the area of brown algae of 1.68 derived from the niche modelled estimates above. |
| Rhodoliths | 0.021–0.23 | Minimum estimate (Moura et al., 2013) and maximum estimate (Carvalho et al., 2020) |
| Total macroalgal area on rocky habitat | 4.78 | |
| Macroalgae on soft/sandy and coral habitat | | |
| *Halimeda* bioherms (along with *Caulerpa*, *Padina* and other green algae) | 1.2 | McNeil et al. (2016) |
| Coral reef-associated macroalgae | 0.038 | Reef area (Spalding & Grenfell, 1997), % cover (Bruno et al., 2009) |
| Total macroalgal area on soft/sandy and coral habitat | 1.24 | |
| Floating macroalgae | | |
| Floating wild populations | | |
| Floating brown algae (*Sargassum* sp.) | 0.050 | Atlantic (Wang et al., 2019) and Chinese (Qi et al., 2017; Zhang et al., 2019) golden tides. Minimum estimate. |
| Floating green algae | 0.001 | Chinese green tides (Liu et al., 2013; Zhang et al., 2019). Minimum estimate |
| Seaweed aquaculture | 0.002 | Global production (Food & Agriculture Organization of the United Nations, 2020), yield (see Duarte et al., 2017, and references therein) |
| Total area of floating macroalgae | 0.053 | |
| Total macroalgal area by habitat type | 6.07 | Sum for rocky, sandy and floating habitats |

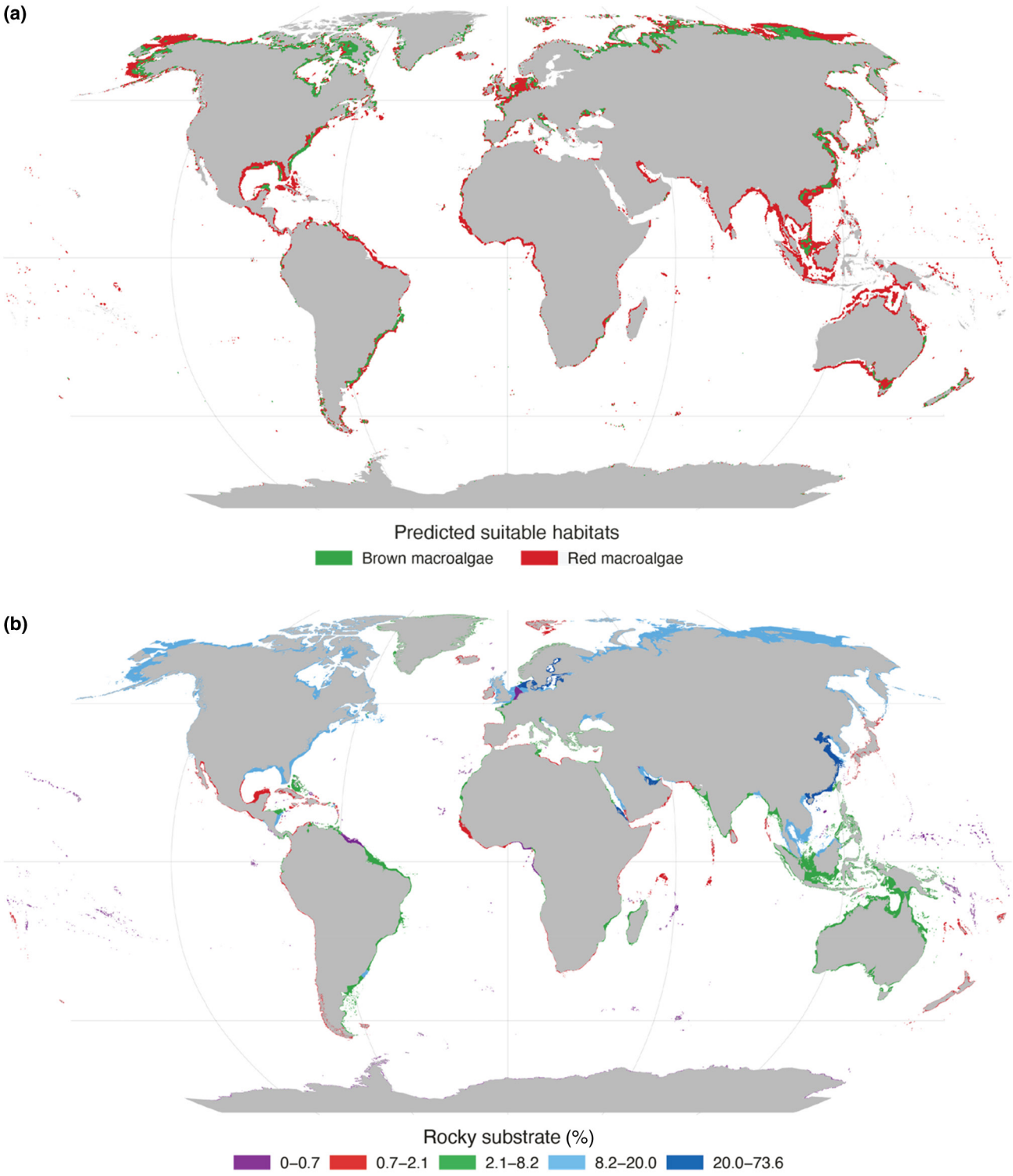


FIGURE 1 (a) Global potential distribution of benthic macroalgae inferred using a global niche model. (b) Global map of the maximum extent of macroalgal distribution, constrained by depths shallower than 50 m and suitable substrate (rocky). The percentage of cliff area is estimated relative to the territorial area of each country (cf. Methods for details)

with species of Desmarestiales also forming algal forests in the Southern Hemisphere. Other genera of brown algae form subtidal forests, including *Cystoseira* (sensu lato, Orellana et al., 2019) in the Mediterranean Sea and adjacent Atlantic Ocean, and *Fucus* in the Baltic Sea. Shade-tolerant red foliose, rhodolith and encrusting algae tend to occupy substrates below brown algal canopies, and dominate in deeper regions with insufficient light for brown algal growth (Gattuso et al., 2006; Vadas & Steneck, 1988).

Other widely distributed macroalgal habitats include canopy-forming brown macroalgae on tropical reefs (e.g. *Sargassum*,

*Turbinaria*), calcifying subtropical and tropical algae, red algal rhodolith habitats, and floating *Sargassum* aggregations. Macroalgae are also found on soft sediments in sheltered locations such as shallow estuaries, lagoons, mudflats, and in seagrass meadows and saltmarshes, where they attach to shells, stones and plants, are free-floating (e.g. the genera *Fucus*, *Ulva*, *Chaetomorpha*, *Gracilaria*, *Ceramium* in cold temperate waters and *Sargassum*, *Turbinaria*, *Udotea*, *Acetabularia* in warm temperate waters), or attached to soft sediments through rhizoids (e.g. *Halimeda*, *Udotea* and *Caulerpa* species in warm temperate and tropical waters and Charophytes in brackish waters worldwide). The macroalgae occurring on or over predominantly soft bottom habitats have been less studied than those on rocky substrates (with the exception of the genus *Caulerpa*), but may occupy large expanses of coastline and be of global biogeochemical significance (Rees et al., 2007). Recently, macroalgal aquaculture has created a new habitat, which is growing at the global scale (Duarte et al., 2021).

The potential distribution of brown algae was predicted with an ecological niche model using the machine learning algorithm boosted regression trees (BRT) to derive the extent of their habitats. The potential distribution of brown algae was also inferred with ecological niche modelling, by combining the machine learning algorithms BRT and adaptive boosting (AdaBoost) using the ensemble technique. The ensemble technique was chosen to reduce the inherent uncertainty of algorithms while at the same time delivering the potential extent of habitat (Araújo & New, 2007). The algorithms fitted the high-resolution environmental layers against georeferenced occurrence records (presences and absences). The predictors chosen were sea bottom temperatures (long-term maximum and minimum), salinity at bottom, nutrients at bottom (such as phosphate and nitrate), permanent sea ice extent and light at bottom, which are expected to develop biological meaningful models for marine forest species (Assis, Araújo, et al., 2018; Neiva et al., 2014). Presence records were compiled from the new fine-tuned global distribution dataset of marine forests (Assis et al., 2020), which provides ~1 million records of the large brown algae Laminariales, Tilopteridales and Fucales (floating species *Sargassum fluitans*, *Sargassum natans* and *Sargassum pusillum* were excluded).

Because BRT and AdaBoost require presence and absence records, and because only presences are available at the scales of our study, a dataset of pseudo-absences was produced using a threshold independent method. Pseudo-absences allow the algorithms to be fed with information of where species do not potentially occur, but their selection criteria can influence explained data variability, final accuracy of predictions and, most importantly, the extent at which models restrict distributions (Chefaoui & Lobo, 2008), particularly when using threshold dependent methods (Chefaoui & Lobo, 2007). The method used followed the three-step approach of randomly generating pseudo-absences within a constrained distance from presences, while considering regions that are environmentally dissimilar from presences (Senay et al., 2013). This is threshold independent, and aimed to capture ecological niches with high predictive performance and to reduce overprediction of area estimates (Assis, Araújo, et al., 2018; Senay et al., 2013). The two first steps used a kernel probability surface developed with the records of occurrence and a spatial grid with the same resolution as the environmental layers, from which pseudo-absences were randomly generated (Senay et al., 2013). This accounted for bias resulting from an unbalanced distribution of occurrence records (Assis, Araújo, et al., 2018; Phillips et al., 2009) and restricted models to the actual distribution of brown algae species (Barve et al., 2011). The third step reduced surplus information by structuring random pseudo-absences with environmental information using the K-means clustering algorithm with the total number of occurrence records as the k parameter (Senay et al., 2013).

The optimal parameters of BRT reducing overfitting (i.e. tree complexity, learning rate, and number of regression trees; Elith & Leathwick, 2011) and AdaBoost (i.e. number of interactions, shrinkage and degrees of freedom; Martins et al., 2021) were tuned with cross-validation by partitioning both presences and pseudo-absences into 10 distinct latitudinal bands (using independent training and testing datasets). Mean area under the curve (AUC) identified the combination of parameters retrieving higher potential for spatial/temporal transferability (Elith & Leathwick, 2011).

Distribution maps were produced per algorithm by reclassifying the output of each model (i.e. probability of occurrence) to a binomial surface reflecting presences and absences with a threshold maximizing AUC. These maps were then ensembled (Araújo & New, 2007) to produce a final predictive map representing the consensus of distributional areas of brown algae. The final performance of the ensemble model was reported with sensitivity (true presence rate), AUC, and true skill statistics (TSS > .8 excellent model accuracy, Allouche et al., 2006). Partial plots were produced to depict the effect of each environmental layer on the response of the models (Elith et al., 2008).

The area of intertidal rocky shore macroalgae was estimated as the product of the global intertidal area ($0.128 \times 10^6$ km$^2$, Murray et al., 2019) and the rocky shore fraction (0.52, Young & Carilli, 2019), further assuming 20% of the rocky shore to be covered by macroalgae. The area of subtidal brown algae was derived from the niche modelling approach corrected for the fraction of shoreline that is rocky (0.52, Young & Carilli, 2019), minus the estimated area of intertidal algae. The area of subtidal red algae was upscaled from the ratio of the area of red algae (extending below the brown algae belt) to brown algae of 1.68 derived from the niche modelled estimates above. The area of rhodoliths was derived using the minimum (Moura et al., 2013) and maximum (Carvalho et al., 2020) estimates reported in the literature (Table 1).

The area of macroalgae over soft sediments was calculated as the area of *Halimeda* bioherms, and the area of macroalgae on coral reefs was derived as the product of the global coral reefs area and the reported percent algal cover (Table 1). The area of floating macroalgae was derived from the reported area of floating *Sargassum* species and green algae and the area of farmed seaweed (Table 1).

## 2.2 | NPP estimates by habitat type

We compiled estimates of macroalgae NPP using grey literature, peer-reviewed studies and personal unpublished data (see Pessarrodona et al., 2021 for details and Pessarrodona, Filbee-Dexter, Krumhansl, Pedersen, et al., 2021 for the database). To be included in our compilation, studies had to fit the following criteria: first, studies had to examine macroalgae NPP on a per area basis. Second, studies had to provide estimates of NPP at the primary producer level with minimal interference of heterotrophic organisms (i.e. net ecosystem primary production was not included). Third, studies had to capture seasonal variability in NPP throughout the year, with studies conducted at a single point in time, month or season not being included (with the exception of studies concerning annual species where the growth or biomass accumulation was measured at the end of their life cycle). Fourth, quantification of productivity had to be performed in situ on the reef or outdoor mesocosms mimicking natural reef conditions. Fifth, details of the specific sampling location and measuring method had to be provided. Sixth, studies had to provide new data not previously reported in other publications. After applying the criteria above, our final filtered dataset featured 229 independent studies published between 1967 and 2020.

Available data were extracted from text, tables, figures or supplementary material in the articles. In our study, a record was considered to be the areal net primary productivity of a taxon over the course of a year. If a study reported NPP from multiple taxa, depths, sites, methods or time points, these were entered as separate case studies (separate rows). If the data were not directly reported as annual rates, these were computed based on the monthly, bimonthly or seasonal means, with the corresponding standard deviation also being computed. Data were entered into the template in the same units as the original source, but were also standardized to annual areal carbon production (i.e. g C/$m^2$/year). Values reported in fresh or dry weight (FW, DW respectively) were converted to carbon using species- and genus- (most cases) or family- and order-specific factors when these were not available for a given species. Conversion factors provided in the studies were preferably used, but otherwise these were derived from the database provided in Brey et al. (2010). Metadata describing the depth, substrate, sampling year and season, taxonomy, study site and its geolocation, measuring method and data extraction procedure were attached to each individual row (Pessarrodona, Filbee-Dexter, Krumhansl, Moore, et al., 2021).

Given that estimates covered a wide range of algal forms, habitats and depths, the methods used to estimate NPP varied across studies. These fell into three basic approaches: measurements of production using diel changes in dissolved oxygen inside photorespirometry chambers, and estimates based on changes of accumulated biomass – either through periodic harvests of entire plants, or by following increases in individual plant biomass (e.g. through tagging, staining or punching holes). A total of 87% of the records compiled used biomass-accumulation-based methods, which generally measure the carbon exclusively destined to thallus growth and are therefore underestimates of NPP since they do not account for assimilated carbon lost through exudation.

The final dataset featured measurements from 229 species from 49 families and 26 orders, encompassing all major seaweed groups and functional forms (sensu Steneck & Dethier, 1994). This included all the major genera of canopy forming brown algae (e.g. *Fucus*, *Ascophyllum*, *Laminaria*, *Ecklonia*, *Macrocystis*), as well as the principal primary producers in coral reefs (algal turfs and *Sargassum* spp.) (Table S5). Measurements were classified into habitat categories defined based on vegetation structure (forming forests, beds, nodules or mounds), substrate (coral or rocky reef), the dominant vegetation (e.g. brown, red or green algae) as well as their position within the water column (benthic or pelagic). These were: rhodolith beds, *Halimeda* bioherms, subtidal (rocky reef) brown algae, subtidal deep (rocky reef) red algae, coral reef-associated algae, intertidal algae, floating brown algae (*Sargassum*) and floating green algae (referred to as green tides) (Pessarrodona, Filbee-Dexter, Krumhansl, Moore, et al., 2021). Measurements were obtained from a total of 420 individual sites distributed on all continents from the intertidal to 55 m depth (Pessarrodona, Filbee-Dexter, Krumhansl, Moore, et al., 2021), although the majority of measurements were conducted at shallow depths and in subtidal brown algae, coral-reef associated algae, and intertidal habitats (Pessarrodona, Filbee-Dexter, Krumhansl, Moore, et al., 2021).

To calculate the mean of NPP by each habitat type, we first aggregated the NPP from species belonging to the same sampling area within each habitat type, sampling year, depth, measuring method and study. This yielded the total areal productivity at the plot level (e.g. by summing the NPP of multiple species of brown algae in a *Sargassum* spp. bed). We then averaged estimates within each site and habitat type by pooling across sampling years, depths, measuring methods and studies. In this way, measurements made at different sites had equal weighting in our habitat NPP estimates regardless of the number of observations conducted within a site. We chose this approach as we prioritized equal spatial representation across the areas that supported macroalgae, but not pooling the data produced similar results (Table S6). Finally, the mean and standard deviation of all the sites for a given habitat were calculated.

The NPP for seaweed aquaculture was derived from the global annual yield of 31 million tons FW (Food & Agriculture Organization of the United Nations, 2020), assuming DW to be 10% of FW and carbon to be 24.8% of DW (Duarte et al., 2017). The yield, however, represents a fraction of NPP, as a large fraction is lost in the environment prior to harvest. We then calculated the areal NPP from seaweed aquaculture from a yield of 1,604 tons DW/$km^2$ (Broch et al., 2019) increased by the fraction of NPP lost in the environment, assumed to be 61% (Zhang et al., 2012). The global extent of seaweed aquaculture was calculated from the global yield of 31 million tons FW/year (Food & Agriculture Organization of the United Nations, 2020), adjusted for the areal yield (1,604 tons FW/$km^2$), to estimate the global extent of seaweed aquaculture in 2017 to be about $0.002 \times 10^6$ $km^2$.

The modelled global distribution of seaweed and the dataset on NPP supported by macroalgae are available at https://doi.org/10.6084/m9.figshare.16574822.v2 and https://doi.org/10.6084/m9.figshare.14882322.v1, respectively.

## 3 | RESULTS

### 3.1 | Global macroalgal extent

#### 3.1.1 | Global niche model (approach 1)

We applied a comprehensive niche model to generate an improved global map of potential macroalgal distribution (Figure 1a). When defining the light threshold as the first decile of minimum light requirements for growth (Mineur et al., 2015), this approach generated upper global estimates of $2.63 \times 10^6$ km$^2$ for brown algae, distributed between a subtidal area of $2.50 \times 10^6$ km$^2$ and an intertidal area of $0.13 \times 10^6$ km$^2$. For red algae, the upper limit to their global area is estimated at $7.09 \times 10^6$ km$^2$, with $6.69 \times 10^6$ km$^2$ in the subtidal zone and $0.40 \times 10^6$ km$^2$ in the intertidal. While the brown and red algal areas overlap over much of their distribution, the belt of subtidal red algae extending beyond the brown algal belt is estimated at a maximum of $4.19 \times 10^6$ km$^2$. Overall, we find that the upper limit to the area that red and brown macroalgae occupy is $7.22 \times 10^6$ km$^2$ (Table 1, Figure 1a). This estimate, which does not include habitats dominated by green algae, such as *Halimeda* bioherms, is considerably lower than the absolute maximum estimate of $12.5 \times 10^6$ km$^2$ derived by Gattuso et al. (2020) using similar light thresholds, demonstrating the importance of salinity, nitrogen concentration, temperature and sea ice in constraining macroalgal distribution. Gattuso et al. (2006, 2020) did not include the distribution area of Antarctic macroalgae in their estimate, but that is of minor importance as this constitutes < 0.25% of the global macroalgal area in our model estimates.

#### 3.1.2 | Area of rocky shore shallower than 50 m (approach 2)

We provided an independent estimate of the area macroalgae may occupy on rocky shores from the global distribution of rocky shores (Young & Carilli, 2019) at depths shallower than 50 m (cf. Methods). The resulting map (Figure 1b) yields an upper limit to macroalgal area on rocky shores of $4.9 \times 10^6$ km$^2$ (Table 1). This is below our estimated upper limit of the global macroalgal area of $7.22 \times 10^6$ km$^2$ (Table 1, Figure 1a), which did not consider seafloor characteristics among the constraining factors.

#### 3.1.3 | Global estimates by habitat type (approach 3)

We then proceeded to assess the global macroalgal area by habitat type, including rocky shores, soft bottoms and floating habitats (Table 1). Use of recently developed remote sensing tools, new modelling approaches, intensified research efforts and monitoring surveys in the coastal zone, and collaborative platforms to report observations have greatly increased our knowledge of the global distribution of macroalgae across habitats (Assis et al., 2020; Krumhansl et al., 2016; Mora-Soto et al., 2020), although still limited to an absence–presence basis. The global intertidal area is estimated at $0.13 \times 10^6$ km$^2$ (see Murray et al., 2019), of which 52% may represent the rocky seabed (cf. Methods). The percent of the seafloor occupied by rocky shores required to constrain the global map of the maximum extent of macroalgal distribution (presented in Figure 1b) was further tested and validated using datasets for a number of nations for which the seafloor type is well documented (cf. Methods). These numbers varied substantially between the countries used for validating the models, which implies that a more precise estimation could be developed if more countries had substrate maps of sufficient quality, resolution and coverage. Figure 1b shows the areas of suitable depth and the percentage of rocky seabed estimated relative to the territorial area of each country. The total estimated area of rock using this approach was $5.4 \times 10^6$ km$^2$ (Table 1).

Assuming an algal cover of 20%, we estimate the total rocky intertidal area occupied by intertidal brown and red algae at $0.013 \times 10^6$ km$^2$, which represents a small contribution to the global macroalgal area (Table 1).

Assis et al. (2020) curated ~1 million distribution records from published sources, herbaria and databases of large brown algae species, which we used to fit an ecological niche model by applying high resolution environmental data as forcing, based on the machine learning algorithms boosted regression trees and adaptive boosting (see Methods). The species included in these records comprise canopy-forming kelps and kelp-like species of the orders Laminariales, Tilopteridales, Desmarestiales and Fucales (Bolton, 2010; Wernberg et al., 2019). Given that rocky shores, where these algal groups typically grow, may occupy only 52% of the global shoreline (Young & Carilli, 2019), the ensemble model developed leads to an estimate of the total area covered by subtidal and intertidal brown algal stands of $1.68 \times 10^6$ km$^2$ (Table 1), with individual estimates ranging between $1.43 \times 10^6$ km$^2$ (AdaBoost algorithm) and $1.79 \times 10^6$ km$^2$ (BRT algorithm). This value compares favourably with recent efforts to assess the global extent of kelp habitat, which is estimated at $2.03 \times 10^6$ km$^2$ (Jayathilake & Costello, 2021), and is expected to be lower, considering the highly detailed climate data used (approx. 450 m at the equator).

While red algae were not modelled on the basis of observations, we applied the ratio of subtidal area occupied by brown and red algae of 1.68 derived from the niche modelled 'total macroalgal area' estimates above (Table 1), to estimate the area of subtidal red algal stands on rocky shores extending deeper than the brown algal stands at $2.98 \times 10^6$ km$^2$ (Table 1). Among the red algae, rhodoliths, predominant in subtropical and tropical regions, occupy large areas. Rhodoliths off Brazil alone occupy between 0.021 × and $0.230 \times 10^6$ km$^2$, comprising the world's largest known rhodolith habitat (Carvalho et al., 2020; Moura et al., 2013). The area of rhodoliths off Brazil constitutes a minimum area for these communities (Table 1). By combining the estimates above (intertidal and subtidal brown and subtidal red algae), we calculate that rocky shore habitats support a total macroalgal area of $4.78 \times 10^6$ km$^2$ (Table 1).

Crucially, macroalgae growing on soft sediments also occupy vast areas, despite the general perception that macroalgae are confined

to hard-bottom habitats. Algae growing on coral reefs occupy an estimated area of 0.038 × $10^6$ $km^2$ (Table 1, Table S1). *Halimeda* bioherms (including other calcareous species such as *Padina* sp.) growing in subtropical and tropical soft sediments, are estimated to cover 1.24 × $10^6$ $km^2$ (Table 1). Although this is considerably less than the area on rocky shores, this area is larger than the global area of seagrass, mangroves and saltmarshes combined (Duarte, 2017). Our estimates do not include macroalgae associated with seagrasses and saltmarshes and those in mudflats because these habitats are not generally dominated by macroalgae. However, in any case, these would represent a contribution of about 0.05 × $10^6$ $km^2$, assuming the area of mudflats [0.06 × $10^6$ $km^2$, assessed as global tidal area (Murray et al., 2019) multiplied by the non-rocky fraction, 48% (Young & Carilli, 2019)], the total area of seagrasses (0.35 × $10^6$ $km^2$, Duarte, 2017) and the total area of saltmarsh (0.05 × $10^6$ $km^2$, McOwen et al., 2017) were all covered by 10% macroalgae.

In addition to benthic macroalgal habitats, floating masses of macroalgae are common in several open-ocean regions, including golden tides of *Sargassum* in the Caribbean Sea, the Sargasso Sea, and the wider tropical Atlantic Ocean (Wang et al., 2019), and golden and green tides (e.g. *Ulva*) in Asia (Liu et al., 2013; Qi et al., 2017). Floating macroalgal mats are also a feature of eutrophied coastal habitats elsewhere (Valiela et al., 1997). Lastly, seaweed aquaculture is an emerging new floating habitat, which has already created 0.002 × $10^6$ $km^2$ (Table 1) of area, largely in Asia (Table 1, Table S1), raising the combined area of floating macroalgal habitats to 0.053 × $10^6$ $km^2$.

When all the habitat-based estimates are integrated, the total estimated macroalgal area amounts to 6.06 × $10^6$ $km^2$ (Table 1), close to our estimated upper bound of 7.22 × $10^6$ $km^2$. This implies that most potential macroalgal habitats are occupied.

### 3.2 | Global production of macroalgae

We compiled areal NPP rates across macroalgal habitats from the literature (Figure 2, Table 2; see Pessarrodona, Filbee-Dexter, Krumhansl, Moore, et al., 2021; Pessarrodona, Filbee-Dexter, Krumhansl, Pedersen, et al., 2021 for details and full dataset)

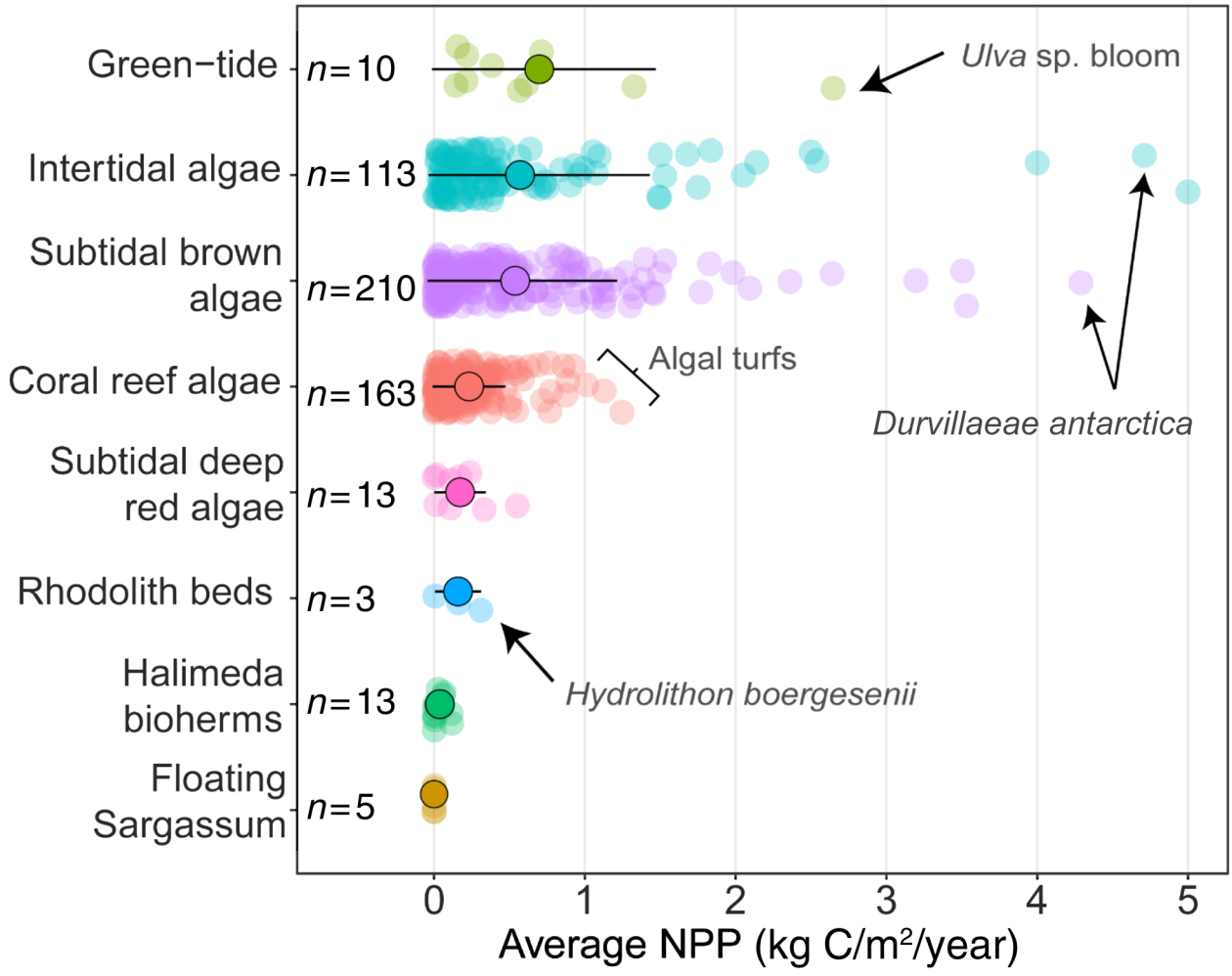


FIGURE 2 Annual net primary productivity for different macroalgal habitat types. Small dots indicate the depth-averaged annual net primary production (NPP) at sites featuring that habitat, while larger dots and error bars indicate the means and standard deviation of each habitat type. The number of site-level measurements for each habitat type is indicated next to each graph (Table 2)

**TABLE 2** Macroalgal net primary production per unit area (NPP, mean, standard deviation and number of site-level estimates), global area and global NPP for the various rocky, soft-bottom and floating macroalgal habitat types for which we reported updated area estimates in Table 1

| | NPP by habitat type (kg C/m$^2$/year) | | | Global area (million km$^2$) | Global NPP (Pg C/year) |
|---|---|---|---|---|---|
| | Mean | *SD* | *n* | | Mean |
| Algae on rocky habitats | | | | | |
| Intertidal communities | 0.587 | 0.818 | 79 | 0.013 | 0.008 |
| Subtidal brown | 0.546 | 0.632 | 142 | 1.680 | 0.917 |
| Subtidal deep red (excl. rhodoliths) | 0.105 | 0.130 | 7 | 2.980 | 0.313 |
| Rhodoliths (max. area) | 0.107 | 0.162 | 4 | 0.230 | 0.025 |
| Total rocky habitat | 0.273 | | | 4.780 | 1.263 |
| Algae on soft/sandy and coral habitat | | | | | |
| *Halimeda* bioherms | 0.038 | 0.040 | 13 | 1.200 | 0.045 |
| Coral reef algae | 0.168 | 0.256 | 78 | 0.038 | 0.006 |
| Total soft/sandy and coral habitat | 0.041 | | | 1.240 | 0.051 |
| Floating macroalgae | | | | | |
| Brown algae (*Sargassum*) | 0.000 | 0.000 | 5 | 0.050 | 0.000 |
| Green algae | 0.472 | 0.326 | 12 | 0.001 | 0.000 |
| Seaweed aquaculture | 1.000 | | | 0.002 | 0.002 |
| Total floating habitat | 0.057 | | | 0.053 | 0.003 |
| Total macroalgae | 0.224 | | | 6.073 | 1.317 |

and multiplied the resulting average values by the estimates of the global extent of these habitats reported above (Approach 3, Table 1). Subtidal brown macroalgal and intertidal macroalgal ecosystems supported similarly large contributions to macroalgal NPP with mean values of 0.54 and 0.59 kg C/m$^2$/year, respectively, and maximum reported site- and annual-averaged values well exceeding 2 kg C/m$^2$/year (Figure 2). Macroalgae floating as green tides were the second most productive habitats with mean NPP of 0.47 kg C/m$^2$/year. Coral reef algae (0.17 kg C/m$^2$/year) and red algal habitats, including rhodoliths and deep subtidal algae (both 0.11 kg C/m$^2$/year), had somewhat lower productivity, while pelagic free-floating *Sargassum* supported the lowest NPP of 0.0002 kg C/m$^2$/year. NPP in seaweed aquaculture was calculated to be about 2 Tg C/year, corresponding to an average NPP of 1 kg C/m$^2$/year (cf. Methods).

We then multiplied the estimated area of different macroalgal habitats by their mean NPP to yield a habitat-resolved global estimate of total macroalgal NPP of about 1.32 Pg C/year (Table 2). This estimate far exceeds early estimates of 0.03 Pg C/year (De Vooys, 1979) and is towards the centre of the range published more recently (0.127–2.9 Pg C/year; Duarte, 2017).

## 4 | DISCUSSION

The estimates compiled here lead to a global macroalgal area of 6.06 × 10$^6$ km$^2$ (most likely estimates), and an upper bound of 7.22 × 10$^6$ km$^2$. The global area estimated here lacks an assessment of uncertainty, as the habitat-specific values added to yield the total global area lack error estimates. We provide, however, a range around our area estimate for brown algae derived from niche modelling (mean area 1.68, range 1.43–1.79 × 10$^6$ km$^2$, Table 1). By combining estimates of global area with estimates for NPP for different macroalgal habitats, we derive a global NPP estimate of about 1.32 Pg C/year.

The area of documented macroalgal habitats has increased markedly over recent years, reflecting discoveries of previously uncharted macroalgal habitats. For instance, the largest reported rhodolith area of 0.021–0.23 × 10$^6$ km$^2$ off Brazil is a recent finding, resulting from the discovery of a major mesotrophic reef off the Amazon River (Carvalho et al., 2020; Moura et al., 2013) (Table 1). Climatic refugia for kelps have been recently found at seamounts/oceanic islands and other upwelling areas (Assis, Araújo, et al., 2018) and tropical deep water kelp refugia have also been discovered across the ocean with a potential area of 0.023 × 10$^6$ km$^2$, as revealed by niche modelling (Graham et al., 2007). Enhanced efforts at exploring Arctic macroalgal habitats also recently revealed that kelps grow much deeper in Greenland than previously thought (down to 60 m compared to earlier estimates of 40 m, Krause-Jensen et al., 2019). This finding is significant, because the Arctic represents 34% of the global shoreline (Lantuit et al., 2012), much of which includes rocky bottoms suitable for macroalgal growth (Krause-Jensen & Duarte, 2014). Developments in remote sensing allowing floating macroalgal mats to be resolved are also now contributing more precise global estimates of the area and standing stock of floating macroalgal masses in China (Chen et al., 2019) and the Sargasso Sea (Wang et al., 2019).

Our efforts at calculating global macroalgal NPP are based on a more thorough approach than previous estimates, combining areas and NPP per macroalgal habitat type and, therefore, more transparent and reproducible (Table 2; Pessarrodona, Filbee-Dexter, Krumhansl, Pedersen, et al., 2021; Pessarrodona, Filbee-Dexter, Krumhansl, Moore, et al., 2021). Our estimate represents a first-order estimate, it is an important step towards unpacking the role macroalgae play in the carbon cycle, although further efforts are needed to improve the spatial and temporal resolution of macroalgal NPP fluxes. While our compilation incorporated measurements from across the globe, there was still a geographic bias in the number of measurements, with more study sites being clustered in the Northern Hemisphere (e.g. North Atlantic and Japan). Further, deep and challenging-to-study habitats featured a limited number of NPP measurements, which may not be entirely representative across the global extent of these habitats. In addition, available NPP estimates for macroalgae communities do not represent random samples, and are likely to target relatively well-conserved, high cover stands near major research institutions. Although we cannot discount that such sampling biases and shortcomings contributed error and uncertainty to our estimates, our study is based on the most robust collation of NPP measurements assembled so far, and therefore represents the most up-to-date knowledge on the global NPP of macroalgae. Improving beyond our estimates will require massive, concerted efforts, while conducting truly average assessments of macroalgae NPP will require accurate mapping of macroalgae by community type and an approach to measurement that applies equally and can be conducted remotely, such as remote sensing estimates of NPP, which are possible for phytoplankton, but not for macroalgal communities.

We, however, acknowledge that our estimate of global macroalgal NPP carries significant uncertainties as (a) it does not consider the production of red algal understories in brown algal forests; (b) it does not include macroalgal contributions to NPP in other habitats, such as mudflats, seagrass meadows and saltmarshes, although these likely constitute a very small fraction of the total global NPP of macroalgae; (c) most (77%) of the NPP estimates were derived from biomass harvest or blade-elongation assessments, which do not account for the production lost as particulate and dissolved detritus; (d) the 20% cover in the intertidal zone is likely an underestimate for sheltered rocky shores; (e) our area estimates are binary, that is, either occupied or not by seaweed, implying macroalgal cover to be 100% where present, whereas suitable habitat is unlikely to be fully occupied, as sea urchin barrens devoid of macroalgae caused by overgrazing and other factors often lead to potentially suitable habitat being temporarily free of macroalgal growth; and (f) NPP estimates for seaweed stands available in the literature are not a random sample and are likely to be biased towards stands of high cover. Although our compilation of macroalgal NPP is 10-fold greater than any previous compilation, the data gaps highlighted above provide directions of further work needed to improve our estimate. Amending global environmental datasets with estimates of wave action and substrate type will allow the development of improved models of algal cover and NPP. Reporting algal cover, not only presence–absence, will be important to improve further estimates to yield predictions of macroalgal cover, which would allow NPP to be scaled to the predicted cover.

Given a reported NPP for marine phytoplankton of 47 Pg C/year (Dunne et al., 2007; Field et al., 1998), we calculate that macroalgae contribute at least 3% of global marine NPP, but at least 20% of coastal NPP, where phytoplankton contributes 6.5 Pg C/year (Dunne et al., 2007). We, therefore, argue that future descriptions of the global ocean C cycle, which currently only account for phytoplankton production (Ciais et al., 2014), should be amended to include macroalgal production, as well as the smaller amount of production contributed by other vegetated coastal ecosystems (i.e. seagrass, saltmarsh and mangroves). In addition, estimates of carbon sequestration by blue carbon habitats should include macroalgal forests as well, given the potential for their production to be exported to and trapped within carbon storage habitats and the deep sea where sequestration can readily take place (Krause-Jensen & Duarte, 2016; Ortega et al., 2019; Smale et al., 2018). The estimates presented here highlight that macroalgae and coastal vegetated ecosystems are important components of the global ocean carbon cycle that should not be ignored in future assessments.

The assessment above implies that existing global NPP estimates of about 100 Pg C/year, integrating contributions by oceanic plankton and land vegetation alone (Field et al., 1998), should be increased by 1.5% when including the contribution of marine macroalgae. Indeed, macroalgae contribute about 3% of global marine NPP and 20% of coastal NPP. This represents a significant contribution, of a comparable magnitude in area and NPP to that of the Amazon forest. The area of the Amazon forest is reported at between $6.77 \times 10^6$ km$^2$ (Doughty et al., 2015) and $7.8 \times 10^6$ km$^2$ (Rödig et al., 2018), which combined with an estimated NPP of 4.3 tons C/ha/year (Rödig et al., 2018), yields a NPP of 2.9–3.4 Pg C/year, twice that reported here for macroalgae (Table 2). Macroalgae also contribute to oceanic carbon sequestration through production exported and buried in marine sediments and the deep sea (Krause-Jensen & Duarte, 2016; Krumhansl & Scheibling, 2012; Ortega et al., 2019; Queirós et al., 2019). Indeed, Krause-Jensen & Duarte (2016) calculated that the carbon sequestration supported by macroalgae matches the combined contribution by seagrass meadows, saltmarshes and mangroves.

### 4.1 | Are macroalgal extent and production changing at the global scale?

Changes in the global extent and productivity of macroalgae may impact global carbon cycling and possibly climate change if their net $CO_2$ removal is reduced or increased as a result (Pessarrodona et al., 2018). Moreover, even in the absence of changes in area and production, the contribution of macroalgae to C fluxes may change

if transport to sink sites or the preservation therein are altered. Lack of evidence for global-scale changes in macroalgal NPP led to the argument that macroalgae have a limited, or no, role in climate change regulation (Orr & Sarmiento, 1992), with the consequence that these important components of the biosphere have since been ignored in the climate change debate.

Ocean acidification is generally considered to be beneficial to some non-calcifying macroalgal species because of the scope for increased photosynthetic rates with elevated $CO_2$ concentrations (Kroeker et al., 2013). Ocean acidification has also been invoked to favour, together with warming, the replacement of kelps by turf algae (Connell & Russell, 2010). Recent evidence suggests that ocean acidification may also lead to higher C : N ratios in the tissue of some Laminariales, which in turn may enhance carbon burial rates (Ravaglioli et al., 2019). Hence, the possibility that ocean acidification, warming and other global stressors affect the fraction of macroalgal production sequestered needs be resolved.

There is growing concern that macroalgal forests have experienced environmental changes affecting their capacity for carbon fixation and export (Krumhansl et al., 2016). These changes include the replacement of kelp forests by algal turfs (Filbee-Dexter & Wernberg, 2018), the loss of fucoids [e.g. Mediterranean *Cystoseira* forests (Thibaut et al., 2005) and Atlantic *Fucus* stands (Mineur et al., 2015; Nicastro et al., 2013)] with warming, and overgrowth of impacted coral reefs by macroalgae and turf algae (Anton et al., 2020; Hughes et al., 2003, 2017), among others. There is now ample evidence that macroalgal distributions are changing globally in response to changing climate (Poloczanska et al., 2013; Smale, 2020) and other human impacts (Wernberg et al., 2019). Tropical regions are experiencing an increase in macroalgae from coral reef degradation (Hughes et al., 2017), the expansion of floating algal mats (Wang & Hu, 2017; Wang et al., 2019), and increases in seaweed aquaculture (Duarte et al., 2021). In the warm-temperate zone, a shift from kelp to turf algae is taking place in many regions, leading to declines in biomass and productivity (Krumhansl et al., 2016; Smale, 2020), while in cold temperate zones macroalgal biomass and production may be expanding somewhat due to green and golden tides (Zhang et al., 2019) and seaweed aquaculture (Food & Agriculture Organization of the United Nations, 2020). Lastly, macroalgae are expanding their distributional ranges poleward and experience increased productivity in polar waters (Krause-Jensen et al., 2020; Krause-Jensen & Duarte, 2014), while range contraction of some macroalgal species with climate change is also being reported (Des et al., 2020). Hence, macroalgae do not conform globally to a single increasing or decreasing trend, but these trends vary across latitudes and habitat types. Moreover, while the impact at the global scale is rather limited, efforts to restore macroalgal communities are accelerating around the world, particularly so in the temperate region (Duarte et al., 2020). Hence, changes in macroalgal area and carbon flux in the tropics and polar regions, where macroalgal cover and production are likely increasing, will have a major influence on the global contribution of macroalgae to carbon fluxes that remains to be quantified.

### 4.2 | Prospects

We report here improved estimates of the global area and NPP of macroalgae, as well as current and projected changes, that address a long-standing gap for this biome and provide an improved basis to assess their global role. There is, however, a need to improve our current understanding of the fate of macroalgal carbon along with actionable human intervention options to influence carbon fluxes, to assess the potential for algal forests to support nature-based solutions for climate change mitigation (Gattuso et al., 2018; Krause-Jensen et al., 2018). Our improved estimates of the global distribution, area and production of macroalgal forests clearly identify them as a major component of the biosphere, of comparable areal extent and production to the Amazon forest, and warrant their inclusion in depictions of the global carbon budget.

## ACKNOWLEDGMENTS

We thank Chris Jenkins at the Institute of Arctic & Alpine Research (INSTAAR), University of Colorado at Boulder, USA, and Eleonora Manca at the Joint Nature Conservation Committee, UK, for providing substrate data for the evaluation of the global map of the maximum extent of macroalgal distribution.

## CONFLICT OF INTEREST

The authors declare no conflict of interest.

## DATA AVAILABILITY STATEMENT

Predictive layers of the distribution of macroalgal forests as well as NPP data collected are available at https://doi.org/10.6084/m9.figshare.16574822.v2 and https://doi.org/10.6084/m9.figshare.14882322.v1, respectively.

## ORCID

*Carlos M. Duarte* https://orcid.org/0000-0002-1213-1361
*Jorge Assis* https://orcid.org/0000-0002-6624-4820

## REFERENCES

Allouche, O., Tsoar, A., & Kadmon, R. (2006). Assessing the accuracy of species distribution models: Prevalence, kappa and the true skill statistic (TSS). *Journal of Applied Ecology*, *43*(6), 1223–1232. https://doi.org/10.1111/j.1365-2664.2006.01214.x

Anton, A., Randle, J. L., Garcia, F. C., Rossbach, S., Ellis, J. I., Weinzierl, M., & Duarte, C. M. (2020). Differential thermal tolerance between algae and corals may trigger the proliferation of algae in coral reefs. *Global Change Biology*, *26*(8), 4316–4327. https://doi.org/10.1111/gcb.15141

Araújo, M. B., & New, M. (2007). Ensemble forecasting of species distributions. *Trends in Ecology and Evolution*, *22*, 42–47. https://doi.org/10.1016/j.tree.2006.09.010

Assis, J., Araújo, M. B., & Serrão, E. A. (2018). Projected climate changes threaten ancient refugia of kelp forests in the North Atlantic. *Global Change Biology*, *24*(1), e55–e66. https://doi.org/10.1111/gcb.13818

Assis, J., Fragkopoulou, E., Frade, D., Neiva, J., Oliveira, A., Abecasis, D., Faugeron, S., & Serrão, E. A. (2020). A fine-tuned global distribution

dataset of marine forests. *Scientific Data*, *7*(1), 119. https://doi.org/10.1038/s41597-020-0459-x

Assis, J., Serrão, E. A., Claro, B., Perrin, C., & Pearson, G. A. (2014). Climate-driven range shifts explain the distribution of extant gene pools and predict future loss of unique lineages in a marine brown alga. *Molecular Ecology*, *23*(11), 2797–2810. https://doi.org/10.1111/mec.12772

Assis, J., Serrão, E. Á., Coelho, N. C., Tempera, F., Valero, M., & Alberto, F. (2018). Past climate changes and strong oceanographic barriers structured low-latitude genetic relics for the golden kelp Laminaria ochroleuca. *Journal of Biogeography*, *45*(10), 2326–2336. https://doi.org/10.1111/jbi.13425

Assis, J., Tyberghein, L., Bosch, S., Verbruggen, H., Serrão, E. A., & De Clerck, O. (2017). Bio-ORACLE v2.0: Extending marine data layers for bioclimatic modelling. *Global Ecology and Biogeography*, *27*(3), 277–284. https://doi.org/10.1111/geb.12693

Barve, N., Barve, V., Jiménez-Valverde, A., Lira-Noriega, A., Maher, S. P., Peterson, A. T., Soberón, J., & Villalobos, F. (2011). The crucial role of the accessible area in ecological niche modeling and species distribution modeling. *Ecological Modelling*, *222*(11), 1810–1819. https://doi.org/10.1016/j.ecolmodel.2011.02.011

Bennett, S., Wernberg, T., Connell, S. D., Hobday, A. J., Johnson, C. R., & Poloczanska, E. S. (2016). The 'Great Southern Reef': Social, ecological and economic value of Australia's neglected kelp forests. *Marine and Freshwater Research*, *67*(1), 47–56. https://doi.org/10.1071/MF15232

Blamey, L. K., & Bolton, J. J. (2018). The economic value of South African kelp forests and temperate reefs: Past, present and future. *Journal of Marine Systems*, *188*, 172–181. https://doi.org/10.1016/j.jmarsys.2017.06.003

Bolton, J. J. (2010). The biogeography of kelps (Laminariales, Phaeophyceae): A global analysis with new insights from recent advances in molecular phylogenetics. *Helgoland Marine Research*, *64*(4), 263–279. https://doi.org/10.1007/s10152-010-0211-6

Bostock, H., Jenkins, C., Mackay, K., Carter, L., Nodder, S., Orpin, A., Pallentin, A., & Wysoczanski, R. (2018). Distribution of surficial sediments in the ocean around New Zealand/Aotearoa. Part B: Continental shelf. *New Zealand Journal of Geology and Geophysics*, *62*(1), 24–45. https://doi.org/10.1080/00288306.2018.1523199

Brey, T., Müller-Wiegmann, C., Zittier, Z. M. C., & Hagen, W. (2010). Body composition in aquatic organisms — A global data bank of relationships between mass, elemental composition and energy content. *Journal of Sea Research*, *64*(3), 334–340. https://doi.org/10.1016/j.seares.2010.05.002

Broch, O. J., Alver, M. O., Bekkby, T., Gundersen, H., Forbord, S., Handå, A., Skjermo, J., & Hancke, K. (2019). The kelp cultivation potential in coastal and offshore regions of Norway. *Frontiers in Marine Science*, *5*(529). https://doi.org/10.3389/fmars.2018.00529

Bruno, J. F., Sweatman, H., Precht, W. F., Selig, E. R., & Schutte, V. G. W. (2009). Assessing evidence of phase shifts from coral to macroalgal dominance on coral reefs. *Ecology*, *90*(6), 1478–1484. https://doi.org/10.1890/08-1781.1

Bulleri, F., Eriksson, B. K., Queirós, A., Airoldi, L., Arenas, F., Arvanitidis, C., Bouma, T. J., Crowe, T. P., Davoult, D., Guizien, K., Iveša, L., Jenkins, S. R., Michalet, R., Olabarria, C., Procaccini, G., Serrão, E. A., Wahl, M., & Benedetti-Cecchi, L. (2018). Harnessing positive species interactions as a tool against climate-driven loss of coastal biodiversity. *PLoS Biology*, *16*(9), e2006852. https://doi.org/10.1371/journal.pbio.2006852

Buonomo, R., Chefaoui, R. M., Lacida, R. B., Engelen, A. H., Serrão, E. A., & Airoldi, L. (2018). Predicted extinction of unique genetic diversity in marine forests of *Cystoseira* spp. *Marine Environmental Research*, *138*, 119–128. https://doi.org/10.1016/j.marenvres.2018.04.013

Burrows, M. T., Fox, C. J., Moore, P., Smale, D., Sotheran, I., Benson, A., Greenhill, L., Martino, S., Parker, A., Thompson, E., & Allen, C. J. (2018). Wild seaweed harvesting as a diversification opportunity for fishermen. A report by SRSL for HIE. SAMS Research Services, Ltd. pp. 171.

Bustamante, R. H., Branch, G. M., Eekhout, S., Robertson, B., Zoutendyk, P., Schleyer, M., Dye, A., Hanekom, N., Keats, D., Jurd, M., & McQuaid, C. (1995). Gradients of intertidal primary productivity around the coast of South Africa and their relationships with consumer biomass. *Oecologia*, *102*(2), 189–201. https://doi.org/10.1007/BF00333251

Carpenter, R. C., Hackney, J. M., & Adey, W. H. (1991). Measurements of primary productivity and nitrogenase activity of coral reef algae in a chamber incorporating oscillatory flow. *Limnology and Oceanography*, *36*(1), 40–49. https://doi.org/10.4319/lo.1991.36.1.0040

Carvalho, V. F., Assis, J., Serrão, E. A., Nunes, J. M., Anderson, A. B., Batista, M. B., Barufi, J. B., Silva, J., Pereira, S. M. B., & Horta, P. A. (2020). Environmental drivers of rhodolith beds and epiphytes community along the South Western Atlantic coast. *Marine Environmental Research*, *154*, 104827. https://doi.org/10.1016/j.marenvres.2019.104827

Castorani, M. C. N., Harrer, S. L., Miller, R. J., & Reed, D. C. (2021). Disturbance structures canopy and understory productivity along an environmental gradient. *Ecology Letters*, *24*, 2192–2206. https://doi.org/10.1111/ele.13849

Chefaoui, R., & Lobo, J. (2007). Assessing the conservation status of an Iberian moth using pseudo-absences. *The Journal of Wildlife Management*, *71*(8), 2507–2516. https://doi.org/10.2193/2006-312

Chefaoui, R. M., & Lobo, J. M. (2008). Assessing the effects of pseudo-absences on predictive distribution model performance. *Ecological Modelling*, *210*(4), 478–486. https://doi.org/10.1016/j.ecolmodel.2007.08.010

Chen, Y.-L., Wan, J.-H., Zhang, J., Ma, Y.-J., Wang, L., Zhao, J.-H., & Wang, Z.-Z. (2019). Spatial-temporal distribution of golden tide based on high-resolution satellite remote sensing in the South Yellow Sea. *Journal of Coastal Research*, *90*(sp1), 221–227. https://doi.org/10.2112/SI90-027.1

Ciais, P., Dolman, A. J., Bombelli, A., Duren, R., Peregon, A., Rayner, P. J., Miller, C., Gobron, N., Kinderman, G., Marland, G., Gruber, N., Chevallier, F., Andres, R. J., Balsamo, G., Bopp, L., Bréon, F.-M., Broquet, G., Dargaville, R., Battin, T. J., … Zehner, C. (2014). Current systematic carbon-cycle observations and the need for implementing a policy-relevant carbon observing system. *Biogeosciences*, *11*(13), 3547–3602. https://doi.org/10.5194/bg-11-3547-2014

Connell, S. D., & Russell, B. D. (2010). The direct effects of increasing $CO_2$ and temperature on non-calcifying organisms: Increasing the potential for phase shifts in kelp forests. *Proceedings of the Royal Society B: Biological Sciences*, *277*(1686), 1409–1415. https://doi.org/10.1098/rspb.2009.2069

De Vooys, C. G. (1979). Primary production in aquatic environments. The global carbon cycle. In B. Bolin, E. T. Degens, S. Kempe, & P. Ketner (Eds.), *Scientific Committee on Problems of the Environment (SCOPE) of the International Council of Scientific Unions (ICSU)* (pp. 259–292). Wiley.

Des, M., Martínez, B., DeCastro, M., Viejo, R. M., Sousa, M. C., & Gómez-Gesteira, M. (2020). The impact of climate change on the geographical distribution of habitat-forming macroalgae in the Rías Baixas. *Marine Environmental Research*, *161*, 105074. https://doi.org/10.1016/j.marenvres.2020.105074

Doughty, C. E., Metcalfe, D. B., Girardin, C. A. J., Amézquita, F. F., Cabrera, D. G., Huasco, W. H., & Malhi, Y. (2015). Drought impact on forest carbon dynamics and fluxes in Amazonia. *Nature*, *519*(7541), 78–82. https://doi.org/10.1038/nature14213

Duarte, C. M. (2017). Reviews and syntheses: Hidden forests, the role of vegetated coastal habitats in the ocean carbon budget. *Biogeosciences*, *14*(2), 301–310. https://doi.org/10.5194/bg-14-301-2017

Duarte, C. M., Agusti, S., Barbier, E., Britten, G. L., Castilla, J. C., Gattuso, J. P., Fulweiler, R. W., Hughes, T. P., Knowlton, N., Lovelock, C. E., Lotze, H. K., Predragovic, M., Poloczanska, E., Roberts, C., & Worm, B. (2020). Rebuilding marine life. *Nature*, *580*, 39–51. https://doi.org/10.1038/s41586-020-2146-7

Duarte, C. M., Bhrunn, A., & Krause-Jensen, D. (2021). A seaweed aquaculture imperative to meet global sustainability targets. *Nature Sustainability*, *5*(3), 185–193. https://doi.org/10.1038/s41893-021-00773-9

Duarte, C. M., & Cebrián, J. (1996). The fate of marine autotrophic production. *Limnology and Oceanography*, *41*(8), 1758–1766. https://doi.org/10.4319/lo.1996.41.8.1758

Duarte, C. M., Losada, I. J., Hendriks, I. E., Mazarrasa, I., & Marba, N. (2013). The role of coastal plant communities for climate change mitigation and adaptation. *Nature Climate Change*, *3*(11), 961–968. https://doi.org/10.1038/nclimate1970

Duarte, C. M., Wu, J., Xiao, X., Bruhn, A., & Krause-Jensen, D. (2017). Can seaweed farming play a role in climate change mitigation and adaptation? *Frontiers in Marine Science*, *4*(100). https://doi.org/10.3389/fmars.2017.00100

Dunne, J. P., Sarmiento, J. L., & Gnanadesikan, A. (2007). A synthesis of global particle export from the surface ocean and cycling through the ocean interior and on the seafloor. *Global Biogeochemical Cycles*, *21*(4). https://doi.org/10.1029/2006gb002907

Elith, J., & Leathwick, J. (2011). Boosted Regression Trees for ecological modeling. R Documentation (pp. 1–22). http://www2.uaem.mx/r-mirror/web/packages/dismo/vignettes/brt.pdf

Elith, J., Leathwick, J. R., & Hastie, T. (2008). A working guide to boosted regression trees. *Journal of Animal Ecology*, *77*(4), 802–813. https://doi.org/10.1111/j.1365-2656.2008.01390.x

Estes, J. A., & Palmisano, J. F. (1974). Sea otters: Their role in structuring nearshore communities. *Science*, *185*(4156), 1058–1060. https://doi.org/10.1126/science.185.4156.1058

Field, C. B., Behrenfeld, M. J., Randerson, J. T., & Falkowski, P. (1998). Primary production of the biosphere: Integrating terrestrial and oceanic components. *Science*, *281*(5374), 237–240. https://doi.org/10.1126/science.281.5374.237

Filbee-Dexter, K. (2016). Distribution and abundance of benthic habitats within the sambro ledges ecologically and biologically significant area. *Canadian Technical Report of Fisheries and Aquatic Sciences* (Vol. *3190*, pp. 26). Fisheries and Oceans Canada.

Filbee-Dexter, K., & Wernberg, T. (2018). Rise of turfs: A new battlefront for globally declining kelp forests. *BioScience*, *68*(2), 64–76. https://doi.org/10.1093/biosci/bix147

Food & Agriculture Organization of the United Nations (2020). *The state of world fisheries and aquaculture. Sustainability in action*. Food & Agriculture Organization of the United Nations.

Froehlich, H. E., Afflerbach, J. C., Frazier, M., & Halpern, B. S. (2019). Blue growth potential to mitigate climate change through seaweed offsetting. *Current Biology*, *29*(18), 3087–3093.e3083. https://doi.org/10.1016/j.cub.2019.07.041

Gattuso, J.-P., Gentili, B., Antoine, D., & Doxaran, D. (2020). Global distribution of photosynthetically available radiation on the seafloor. *Earth System Science Data Discussions*, *12*, 1697–1709. https://doi.org/10.5194/essd-2020

Gattuso, J.-P., Gentili, B., Duarte, C. M., Kleypas, J. A., Middelburg, J. J., & Antoine, D. (2006). Light availability in the coastal ocean: Impact on the distribution of benthic photosynthetic organisms and contribution to primary production. *Biogeosciences Discussions*, *3*(4), 895–959.

Gattuso, J.-P., Magnan, A. K., Bopp, L., Cheung, W. W. L., Duarte, C. M., Hinkel, J., Mcleod, E., Micheli, F., Oschlies, A., Williamson, P., Billé, R., Chalastani, V. I., Gates, R. D., Irisson, J.-O., Middelburg, J. J., Pörtner, H.-O., & Rau, G. H. (2018). Ocean solutions to address climate change and its effects on marine ecosystems. *Frontiers in Marine Science*, *5*(337). https://doi.org/10.3389/fmars.2018.00337

GEBCO. (2019). GEBCO 2019 Grid. https://doi.org/10.5285/836f016a-33be-6ddc-e053-6c86abc0788e

Gorman, D., Bajjouk, T., Populus, J., Vasquez, M., & Ehrhold, A. (2013). Modeling kelp forest distribution and biomass along temperate rocky coastlines. *Marine Biology*, *160*(2), 309–325. https://doi.org/10.1007/s00227-012-2089-0

Graham, M. H., Kinlan, B. P., Druehl, L. D., Garske, L. E., & Banks, S. (2007). Deep-water kelp refugia as potential hotspots of tropical marine diversity and productivity. *Proceedings of the National Academy of Sciences of the United States of America*, *104*(42), 16576–16580. https://doi.org/10.1073/pnas.0704778104

Gregr, E. J., Palacios, D. M., Thompson, A., & Chan, K. M. A. (2019). Why less complexity produces better forecasts: An independent data evaluation of kelp habitat models. *Ecography*, *42*(3), 428–443. https://doi.org/10.1111/ecog.03470

Hughes, T. P., Baird, A. H., Bellwood, D. R., Card, M., Connolly, S. R., Folke, C., Grosberg, R., Hoegh-Guldberg, O., Jackson, J. B. C., Kleypas, J., Lough, J. M., Marshall, P., Nyström, M., Palumbi, S. R., Pandolfi, J. M., Rosen, B., & Roughgarden, J. (2003). Climate change, human impacts, and the resilience of coral reefs. *Science*, *301*(5635), 929–933. https://doi.org/10.1126/science.1085046

Hughes, T. P., Barnes, M. L., Bellwood, D. R., Cinner, J. E., Cumming, G. S., Jackson, J. B. C., Kleypas, J., van de Leemput, I. A., Lough, J. M., Morrison, T. H., Palumbi, S. R., van Nes, E. H., & Scheffer, M. (2017). Coral reefs in the Anthropocene. *Nature*, *546*, 82. https://doi.org/10.1038/nature22901

Jayathilake, D. R. M., & Costello, M. J. (2021). Version 2 of the world map of laminarian kelp benefits from more Arctic data and makes it the largest marine biome. *Biological Conservation*, *257*, 109099. https://doi.org/10.1016/j.biocon.2021.109099

Kearney, M., & Porter, W. (2009). Mechanistic niche modelling: Combining physiological and spatial data to predict species' ranges. *Ecology Letters*, *12*(4), 334–350. https://doi.org/10.1111/j.1461-0248.2008.01277.x

Krause-Jensen, D., Archambault, P., Assis, J., Bartsch, I., Bischof, K., Filbee-Dexter, K., Dunton, K. H., Maximova, O., Ragnarsdottir, S. B., Sejr, M., Simakova, U., Spiridonov, V. A., Wegeberg, S., Winding, M. H. S., & Duarte, C. M. (2020). Imprint of climate change on pan-Arctic marine vegetation. *Frontiers in Marine Science*, *7*, 617324. https://doi.org/10.3389/fmars.2020.617324

Krause-Jensen, D., & Duarte, C. M. (2014). Expansion of vegetated coastal ecosystems in the future Arctic. *Frontiers in Marine Science*, *1*, 77. https://doi.org/10.3389/fmars.2014.00077

Krause-Jensen, D., & Duarte, C. M. (2016). Substantial role of macroalgae in marine carbon sequestration. *Nature Geosciences*, *9*, 737–742. https://doi.org/10.1038/ngeo2790

Krause-Jensen, D., Lavery, P., Serrano, O., Marbà, N., Masque, P., & Duarte, C. M. (2018). Sequestration of macroalgal carbon: The elephant in the Blue Carbon room. *Biology Letters*, *14*(6). https://doi.org/10.1098/rsbl.2018.0236

Krause-Jensen, D., Marbà, N., Sanz-Martin, M., Hendriks, I. E., Thyrring, J., Carstensen, J., Sejr, M. K., & Duarte, C. M. (2016). Long photoperiods sustain high pH in Arctic kelp forests. *Science Advances*, *2*(12), e1501938. https://doi.org/10.1126/sciadv.1501938

Krause-Jensen, D., Sejr, M. K., Bruhn, A., Rasmussen, M. B., Christensen, P. B., Hansen, J. L. S., Duarte, C. M., Bruntse, G., & Wegeberg, S. (2019). Deep penetration of kelps offshore along the west coast of Greenland. *Frontiers in Marine Science*, *6*(375). https://doi.org/10.3389/fmars.2019.00375

Kroeker, K. J., Kordas, R. L., Crim, R., Hendriks, I. E., Ramajo, L., Singh, G. S., Duarte, C. M., & Gattuso, J.-P. (2013). Impacts of ocean acidification on marine organisms: Quantifying sensitivities and interaction with warming. *Global Change Biology*, *19*(6), 1884–1896. https://doi.org/10.1111/gcb.12179

Krumhansl, K. A., Okamoto, D. K., Rassweiler, A., Novak, M., Bolton, J. J., Cavanaugh, K. C., Connell, S. D., Johnson, C. R., Konar, B., Ling, S.

D., Micheli, F., Norderhaug, K. M., Pérez-Matus, A., Sousa-Pinto, I., Reed, D. C., Salomon, A. K., Shears, N. T., Wernberg, T., Anderson, R. J., … Byrnes, J. E. K. (2016). Global patterns of kelp forest change over the past half-century. *Proceedings of the National Academy of Sciences of United States of America*, *113*(48), 13785–13790. https://doi.org/10.1073/pnas.1606102113

Krumhansl, K., & Scheibling, R. E. (2012). Production and fate of kelp detritus. *Marine Ecology Progress Series*, *467*, 281–302. https://doi.org/10.3354/meps09940

Lantuit, H., Overduin, P. P., Couture, N., Wetterich, S., Aré, F., Atkinson, D., Brown, J., Cherkashov, G., Drozdov, D., Forbes, D. L., Graves-Gaylord, A., Grigoriev, M., Hubberten, H.-W., Jordan, J., Jorgenson, T., Ødegård, R. S., Ogorodov, S., Pollard, W. H., Rachold, V., … Vasiliev, A. (2012). The Arctic coastal dynamics database: A new classification scheme and statistics on Arctic permafrost coastlines. *Estuaries and Coasts*, *35*(2), 383–400. https://doi.org/10.1007/s12237-010-9362-6

Liu, F., Pang, S., Chopin, T., Gao, S., Shan, T., Zhao, X., & Li, J. (2013). Understanding the recurrent large-scale green tide in the Yellow Sea: Temporal and spatial correlations between multiple geographical, aquacultural and biological factors. *Marine Environmental Research*, *83*, 38–47. https://doi.org/10.1016/j.marenvres.2012.10.007

Løvås, S. M., & Tørum, A. (2001). Effect of the kelp Laminaria hyperborea upon sand dune erosion and water particle velocities. *Coastal Engineering*, *44*(1), 37–63. https://doi.org/10.1016/S0378-3839(01)00021-7

Macreadie, P. I., Anton, A., Raven, J. A., Beaumont, N., Connolly, R. M., Friess, D. A., Kelleway, J. J., Kennedy, H., Kuwae, T., Lavery, P. S., Lovelock, C. E., Smale, D. A., Apostolaki, E. T., Atwood, T. B., Baldock, J., Bianchi, T. S., Chmura, G. L., Eyre, B. D., Fourqurean, J. W., … Duarte, C. M. (2019). The future of Blue Carbon science. *Nature Communications*, *10*(1), 3998. https://doi.org/10.1038/s41467-019-11693-w

Markager, S., & Sand-Jensen, K. (1992). Light requirements and depth zonation of marine macroalgae. *Marine Ecology Progress Series*, *88*(1), 83–92. https://doi.org/10.3354/meps088083

Martínez, B., Radford, B., Thomsen, M. S., Connell, S. D., Carreño, F., Bradshaw, C. J. A., Fordham, D. A., Russell, B. D., Gurgel, C. F. D., & Wernberg, T. (2018). Distribution models predict large contractions of habitat-forming seaweeds in response to ocean warming. *Diversity and Distributions*, *24*, 1350–1366. https://doi.org/10.1111/ddi.12767

Martins, M. R., Assis, J., & Abecasis, D. (2021). Biologically meaningful distribution models highlight the benefits of the Paris Agreement for demersal fishing targets in the North Atlantic Ocean. *Global Ecology and Biogeography*, *30*(8), 1643–1656. https://doi.org/10.1111/geb.13327

McNeil, M. A., Webster, J. M., Beaman, R. J., & Graham, T. L. (2016). New constraints on the spatial distribution and morphology of the Halimeda bioherms of the Great Barrier Reef, Australia. *Coral Reefs*, *35*(4), 1343–1355. https://doi.org/10.1007/s00338-016-1492-2

McOwen, C., Weatherdon, L., Bochove, J.-W., Sullivan, E., Blyth, S., Zockler, C., Stanwell-Smith, D., Kingston, N., Martin, C., Spalding, M., & Fletcher, S. (2017). A global map of saltmarshes. *Biodiversity Data Journal*, *5*, e11764. https://doi.org/10.3897/BDJ.5.e11764

Melis, R., Ceccherelli, G., Piazzi, L., & Rustici, M. (2019). Macroalgal forests and sea urchin barrens: Structural complexity loss, fisheries exploitation and catastrophic regime shifts. *Ecological Complexity*, *37*, 32–37. https://doi.org/10.1016/j.ecocom.2018.12.005

Mineur, F., Arenas, F., Assis, J., Davies, A. J., Engelen, A. H., Fernandes, F., Malta, E.-J., Thibaut, T., Van Nguyen, T. U., Vaz-Pinto, F., Vranken, S., Serrão, E. A., & De Clerck, O. (2015). European seaweeds under pressure: Consequences for communities and ecosystem functioning. *Journal of Sea Research*, *98*, 91–108. https://doi.org/10.1016/j.seares.2014.11.004

Mora-Soto, A., Palacios, M., Macaya, E., Gómez, I., Huovinen, P., Pérez-Matus, A., Young, M., Golding, N., Toro, M., Yaqub, M., & Macias-Fauria, M. (2020). A high-resolution global map of giant kelp (*Macrocystis pyrifera*) forests and intertidal green algae (Ulvophyceae) with Sentinel-2 imagery. *Remote Sensing*, *12*, 694. https://doi.org/10.3390/rs12040694

Moura, R. L., Secchin, N. A., Amado-Filho, G. M., Francini-Filho, R. B., Freitas, M. O., Minte-Vera, C. V., Teixeira, J. B., Thompson, F. L., Dutra, G. F., Sumida, P. Y. G., Guth, A. Z., Lopes, R. M., & Bastos, A. C. (2013). Spatial patterns of benthic megahabitats and conservation planning in the Abrolhos Bank. *Continental Shelf Research*, *70*, 109–117. https://doi.org/10.1016/j.csr.2013.04.036

Murray, N. J., Phinn, S. R., DeWitt, M., Ferrari, R., Johnston, R., Lyons, M. B., Clinton, N., Thau, D., & Fuller, R. A. (2019). The global distribution and trajectory of tidal flats. *Nature*, *565*(7738), 222–225. https://doi.org/10.1038/s41586-018-0805-8

Neiva, J., Assis, J., Fernandes, F., Pearson, G. A., & Serrão, E. A. (2014). Species distribution models and mitochondrial DNA phylogeography suggest an extensive biogeographical shift in the high-intertidal seaweed *Pelvetia canaliculata*. *Journal of Biogeography*, *41*(6), 1137–1148. https://doi.org/10.1111/jbi.12278

Nellemann, C., Corcoran, E., Duarte, C. M., Valdes, L., De Young, C., Fonseca, L., & Grimsditch, G. (2009). *Blue carbon. A rapid response assessment*. United Nations Environment Programme, GRID-Arendal (pp. 79).

Nicastro, K. R., Zardi, G. I., Teixeira, S., Neiva, J., Serrão, E. A., & Pearson, G. A. (2013). Shift happens: Trailing edge contraction associated with recent warming trends threatens a distinct genetic lineage in the marine macroalga *Fucus vesiculosus*. *BMC Biology*, *11*(1), 6. https://doi.org/10.1186/1741-7007-11-6

Orellana, S., Hernández, M., & Sansón, M. (2019). Diversity of *Cystoseira* sensu lato (Fucales, Phaeophyceae) in the eastern Atlantic and Mediterranean based on morphological and DNA evidence, including *Carpodesmia* gen. emend. and *Treptacantha* gen. emend. *European Journal of Phycology*, *54*(3), 447–465. https://doi.org/10.1080/09670262.2019.1590862

Orr, J. C., & Sarmiento, J. L. (1992). Potential of marine macroalgae as a sink for CO2: Constraints from a 3-D general circulation model of the global ocean. *Water, Air, and Soil Pollution*, *64*(1), 405–421. https://doi.org/10.1007/BF00477113

Ortega, A., Geraldi, N. R., Alam, I., Kamau, A. A., Acinas, S. G., Logares, R., Gasol, J. M., Massana, R., Krause-Jensen, D., & Duarte, C. M. (2019). Important contribution of macroalgae to oceanic carbon sequestration. *Nature Geoscience*, *12*(9), 748–754. https://doi.org/10.1038/s41561-019-0421-8

Pace, M. L., & Lovett, G. M. (2013). Primary production: The foundation of ecosystems. In K. C. Weathers, D. L. Strayer, & G. E. Likens (Eds.), *Fundamentals of ecosystem science* (pp. 27–51). Elsevier.

Pessarrodona, A., Filbee-Dexter, K., Krumhansl, K. A., Pedersen, M. F., Moore, P. J., & Wernberg, T. (2021). A global dataset of seaweed net primary productivity. figshare. [Data set]. https://doi.org/10.6084/m9.figshare.14882322.v1

Pessarrodona, A., Moore, P. J., Sayer, M. D. J., & Smale, D. A. (2018). Carbon assimilation and transfer through kelp forests in the NE Atlantic is diminished under a warmer ocean climate. *Global Change Biology*, *24*, 4386–4398. https://doi.org/10.1111/gcb.14303

Pessarrodona, P., Filbee-Dexter, K., Krumhansl, K. A., Moore, P. J., & Wernberg, T. (2021). A global dataset of seaweed net primary productivity. *bioRxiv* 2021.07.12.452112. https://doi.org/10.1101/2021.07.12.452112

Phillips, S. J., Dudík, M., Elith, J., Graham, C. H., Lehmann, A., Leathwick, J., & Ferrier, S. (2009). Sample selection bias and presence-only

distribution models: Implications for background and pseudo-absence data. *Ecological Applications*, *19*(1), 181–197. https://doi.org/10.1890/07-2153.1

Poloczanska, E. S., Brown, C. J., Sydeman, W. J., Kiessling, W., Schoeman, D. S., Moore, P. J., Brander, K., Bruno, J. F., Buckley, L. B., Burrows, M. T., Duarte, C. M., Halpern, B. S., Holding, J., Kappel, C. V., O'Connor, M. I., Pandolfi, J. M., Parmesan, C., Schwing, F., Thompson, S. A., & Richardson, A. J. (2013). Global imprint of climate change on marine life. *Nature Climate Change*, *3*, 919–925. https://doi.org/10.1038/nclimate1958

Populus, J., Vasquez, M., Albrecht, J., Manca, E., Agnesi, S., Al, H. Z., Andersen, J., Annunziatellis, A., Bekkby, T., Bruschi, A., Doncheva, V., Drakopoulou, V., Duncan, G., Inghilesi, R., Kyriakidou, C., Lalli, F., Lillis, H., Mo, G., Muresan, M., … Tunesi, L. (2017). EUSeaMap, a European broad-scale seabed habitat map. Ifremer. pp. 174.

Qi, L., Hu, C., Wang, M., Shang, S., & Wilson, C. (2017). Floating algae blooms in the East China Sea. *Geophysical Research Letters*, *44*(22), 11501–11509. https://doi.org/10.1002/2017gl075525

Queirós, A. M., Stephens, N., Widdicombe, S., Tait, K., McCoy, S. J., Ingels, J., Rühl, S., Airs, R., Beesley, A., Carnovale, G., Cazenave, P., Dashfield, S., Hua, E. R., Jones, M., Lindeque, P., McNeill, C. L., Nunes, J., Parry, H., Pascoe, C., … Somerfield, P. J. (2019). Connected macroalgal-sediment systems: Blue carbon and food webs in the deep coastal ocean. *Ecological Monographs*, *89*, e01366. https://doi.org/10.1002/ecm.1366

Ravaglioli, C., Bulleri, F., Rühl, S., McCoy, S. J., Findlay, H. S., Widdicombe, S., & Queirós, A. M. (2019). Ocean acidification and hypoxia alter organic carbon fluxes in marine soft sediments. *Global Change Biology*, *25*(12), 4165–4178. https://doi.org/10.1111/gcb.14806

Rees, S. A., Opdyke, B. N., Wilson, P. A., & Henstock, T. J. (2007). Significance of Halimeda bioherms to the global carbonate budget based on a geological sediment budget for the Northern Great Barrier Reef, Australia. *Coral Reefs*, *26*(1), 177–188. https://doi.org/10.1007/s00338-006-0166-x

Rödig, E., Cuntz, M., Rammig, A., Fischer, R., Taubert, F., & Huth, A. (2018). The importance of forest structure for carbon fluxes of the Amazon rainforest. *Environmental Research Letters*, *13*(5), 054013. https://doi.org/10.1088/1748-9326/aabc61

Senay, S. D., Worner, S. P., & Ikeda, T. (2013). Novel three-step pseudo-absence selection technique for improved species distribution modelling. *PLoS One*, *8*(8), e71218. https://doi.org/10.1371/journal.pone.0071218

Serrano, O., Lovelock, C. E., B. Atwood, T., Macreadie, P. I., Canto, R., Phinn, S., Arias-Ortiz, A., Bai, L. E., Baldock, J., Bedulli, C., Carnell, P., Connolly, R. M., Donaldson, P., Esteban, A., Ewers Lewis, C. J., Eyre, B. D., Hayes, M. A., Horwitz, P., Hutley, L. B., … Duarte, C. M. (2019). Australian vegetated coastal ecosystems as global hotspots for climate change mitigation. *Nature Communications*, *10*(1), 4313. https://doi.org/10.1038/s41467-019-12176-8

Smale, D. A. (2020). Impacts of ocean warming on kelp forest ecosystems. *New Phytologist*, *225*, 1447–1454. https://doi.org/10.1111/nph.16107

Smale, D. A., Moore, P. J., Queirós, A. M., Higgs, N. D., & Burrows, M. T. (2018). Appreciating interconnectivity between habitats is key to blue carbon management. *Frontiers in Ecology and the Environment*, *16*(2), 71–73. https://doi.org/10.1002/fee.1765

Smith, S. V. (1981). Marine macrophytes as a global carbon sink. *Science*, *211*(4484), 838–840.

Song, X.-H., Assis, J., Zhang, J., Gao, X., Choi, H.-G., Duan, D.-L., Serrão, E. A., & Hu, Z.-M. (2021). Climate-induced range shifts shaped the present and threaten the future genetic variability of a marine brown alga in the Northwest Pacific. *Evolutionary Applications*, *14*(7), 1867–1879. https://doi.org/10.1111/eva.13247

Spalding, M. D., & Grenfell, A. M. (1997). New estimates of global and regional coral reef areas. *Coral Reefs*, *16*(4), 225–230. https://doi.org/10.1007/s003380050078

Steneck, R. S., & Dethier, M. N. (1994). A functional group approach to the structure of algal-dominated communities. *Oikos*, 476–498.

Steneck, R. S., Graham, M. H., Bourque, B. J., Corbett, D., Erlandson, J. M., Estes, J. A., & Tegner, M. J. (2002). Kelp forest ecosystems: Biodiversity, stability, resilience and future. *Environmental Conservation*, *29*(4), 436–459.

Taguchi, E., Stammer, D., & Zahel, W. (2014). Inferring deep ocean tidal energy dissipation from the global high-resolution data-assimilative HAMTIDE model. *Journal of Geophysical Research: Oceans*, *119*(7), 4573–4592. https://doi.org/10.1002/2013jc009766

Teagle, H., Hawkins, S. J., Moore, P. J., & Smale, D. A. (2017). The role of kelp species as biogenic habitat formers in coastal marine ecosystems. *Journal of Experimental Marine Biology and Ecology*, *492*, 81–98. https://doi.org/10.1016/j.jembe.2017.01.017

Thibaut, T., Pinedo, S., Torras, X., & Ballesteros, E. (2005). Long-term decline of the populations of Fucales (*Cystoseira* spp. and *Sargassum* spp.) in the Albères coast (France, North-western Mediterranean). *Marine Pollution Bulletin*, *50*(12), 1472–1489. https://doi.org/10.1016/j.marpolbul.2005.06.014

Vadas, R. L., & Steneck, R. S. (1988). Zonation of deep water benthic algae in the Gulf of Maine. *Journal of Phycology*, *24*(3), 338–346. https://doi.org/10.1111/j.1529-8817.1988.tb04476.x

Valiela, I., McClelland, J., Hauxwell, J., Behr, P. J., Hersh, D., & Foreman, K. (1997). Macroalgal blooms in shallow estuaries: Controls and ecophysiological and ecosystem consequences. *Limnology and Oceanography*, *42*(5part2), 1105–1118. https://doi.org/10.4319/lo.1997.42.5_part_2.1105

Wahl, M., Schneider Covachã, S., Saderne, V., Hiebenthal, C., Müller, J. D., Pansch, C., & Sawall, Y. (2018). Macroalgae may mitigate ocean acidification effects on mussel calcification by increasing pH and its fluctuations. *Limnology and Oceanography*, *63*(1), 3–21. https://doi.org/10.1002/lno.10608

Wang, M., & Hu, C. (2017). Predicting Sargassum blooms in the Caribbean Sea from MODIS observations. *Geophysical Research Letters*, *44*(7), 3265–3273. https://doi.org/10.1002/2017gl072932

Wang, M., Hu, C., Barnes, B. B., Mitchum, G., Lapointe, B., & Montoya, J. P. (2019). The great Atlantic Sargassum belt. *Science*, *365*(6448), 83–87. https://doi.org/10.1126/science.aaw7912

Wernberg, T., Krumhansl, K., Filbee-Dexter, K., & Pedersen, M. F. (2019). Chapter 3 - Status and trends for the world's kelp forests. In C. Sheppard (Ed.), *World seas: An environmental evaluation* (2nd ed., pp. 57–78). Academic Press.

Whittaker, R. H., & Likens, G. E. (1973). Carbon and the biota. *Brookhaven Symposium in Biology*, *24*, 281–302.

Young, A. P., & Carilli, J. E. (2019). Global distribution of coastal cliffs. *Earth Surface Processes and Landforms*, *44*(6), 1309–1316. https://doi.org/10.1002/esp.4574

Young, M., Ierodiaconou, D., & Womersley, T. (2015). Forests of the sea: Predictive habitat modelling to assess the abundance of canopy forming kelp forests on temperate reefs. *Remote Sensing of Environment*, *170*, 178–187. https://doi.org/10.1016/j.rse.2015.09.020

Zhang, J., Ding, X., Zhuang, M., Wang, S., Chen, L., Shen, H., & He, P. (2019). An increase in new Sargassum (Phaeophyceae) blooms along the coast of the East China Sea and Yellow Sea. *Phycologia*, *58*(4), 374–381. https://doi.org/10.1080/00318884.2019.1585722

Zhang, J., Fang, J., Wang, W., Du, M., Gao, Y., & Zhang, M. (2012). Growth and loss of mariculture kelp Saccharina japonica in Sungo Bay, China. *Journal of Applied Phycology*, *24*(5), 1209–1216. https://doi.org/10.1007/s10811-011-9762-4

## BIOSKETCH

The authors are marine ecologists with a track record of conducting research in coastal ecosystems and, specifically, macroalgal communities from different perspectives including population genetics and dynamics, production, biogeography, and biogeochemical fluxes, as well as responses to climate change.

## SUPPORTING INFORMATION

Additional supporting information may be found in the online version of the article at the publisher's website.

**How to cite this article:** Duarte, C. M., Gattuso J.-P., Hancke K., Gundersen H., Filbee-Dexter K., Pedersen M. F., Middelburg J. J., Burrows M. T., Krumhansl K. A., Wernberg T., Moore P., Pessarrodona A., Ørberg S. B., Pinto I. S., Assis J., Queirós A. M., Smale D. A., Bekkby T., Serrão E. A., & Krause-Jensen D. (2022). Global estimates of the extent and production of macroalgal forests. *Global Ecology and Biogeography*, *00*, 1–18. https://doi.org/10.1111/geb.13515